

Published in final edited form as:

J Neurosci. 2010 September 1; 30(35): 11745–11761. doi:10.1523/JNEUROSCI.1769-10.2010.

Progressive NKCC1-dependent neuronal chloride accumulation during neonatal seizures

Volodymyr I. Dzhalal^{1,5}, Kishore V. Kuchibhotla^{1,3,5}, Joseph C. Glykys¹, Kristopher T. Kahle², Waldemar B. Swiercz¹, Guoping Feng⁴, Thomas Kuner⁴, George J. Augustine⁴, Brian J. Bacskaï¹, and Kevin J. Staley¹

¹Department of Neurology, Massachusetts General Hospital and Harvard Medical School, Boston, MA 02114, USA

²Department of Neurosurgery, Massachusetts General Hospital and Harvard Medical School, Boston, MA 02114, USA

³Program in Biophysics, Harvard University, Cambridge, MA 02138, USA

⁴Department of Neurobiology, Duke University Medical Center, Durham, NC 27710, USA

Abstract

Seizures induce excitatory shifts in the reversal potential for GABA_A receptor-mediated responses, which may contribute to the intractability of electroencephalographic seizures and preclude the efficacy of widely-used GABAergic anticonvulsants such as phenobarbital. We now report that in intact hippocampi prepared from neonatal rats and transgenic mice expressing Clomeleon, recurrent seizures progressively increase the intracellular chloride concentration ($[Cl^-]_i$) assayed by Clomeleon imaging and invert the net effect of GABA_A receptor activation from inhibition to excitation assayed by the frequency of action potentials and intracellular Ca²⁺ transients. These changes correlate with increasing frequency of seizure-like events and reduction in phenobarbital efficacy. The Na⁺-K⁺-2Cl⁻ (NKCC1) co-transporter blocker bumetanide inhibited seizure-induced neuronal Cl⁻ accumulation and the consequent facilitation of recurrent seizures. Our results demonstrate a novel mechanism by which seizure activity leads to $[Cl^-]_i$ accumulation, thereby increasing the probability of subsequent seizures. This provides a potential mechanism for the early crescendo phase of neonatal seizures.

Keywords

GABA; Phenobarbital; Clomeleon; action potential; epileptiform activity; hippocampus

Introduction

Neurons respond to a variety of stimuli with long-term shifts in the reversal potential for GABA_A receptor-mediated postsynaptic currents (E_{GABA}). For example, epileptogenic injuries alter neuronal chloride transport, which is the principal determinant of E_{GABA} (Jin et al., 2005; Pathak et al., 2007). E_{GABA} is persistently shifted to more positive (depolarizing) potentials by prolonged seizure activity (Khalilov et al., 2003) or trains of

Corresponding Author: Dr. Kevin J. Staley Dept. of Neurology, MIND, MGH 16th St., CNY B-114, Rm. 2600 Charlestown, MA 02129 Phone: 617.643.0363; Fax: 617.643.0141 kstaley@partners.org.

⁵These authors contributed equally to this work

Supplemental Data. Supplemental Data include five figures and are available online.

action potentials without (Fiumelli and Woodin, 2007; Brumback and Staley, 2008) or with concomitant GABA_A receptor activation (Woodin et al., 2003). In addition, other events including oxygen-glucose deprivation (Pond et al., 2006) and trauma (van den Pol et al., 1996) shift E_{GABA} to more depolarized potentials. Depolarized values of E_{GABA} reduce the efficacy of inhibition and contribute to seizure activity (Dzhala and Staley, 2003; Khazipov et al., 2004; Dzhala et al., 2005).

Immature neurons express high levels of NKCC1 (Delpire, 2000; Wang et al., 2002; Dzhala et al., 2005), an electro-neutral co-transporter that imports Na⁺, K⁺ and Cl⁻. This raises the intracellular chloride concentration, resulting in a depolarized E_{GABA}. This shift in E_{GABA} can initiate a positive feedback cycle in neonatal seizures (Staley and Smith, 2001), and depolarized values of E_{GABA} contribute to the reduced efficacy of GABA-enhancing anticonvulsants (Dzhala et al., 2005; Dzhala et al., 2008) that are first-line agents in the treatment of neonatal seizures (Rennie and Boylan, 2003; Carmo and Barr, 2005). NKCC1 is selectively blocked by low micromolar concentrations of the loop diuretic bumetanide (Isenring et al., 1998; Hannaert et al., 2002). By reducing intracellular chloride accumulation, this diuretic shifts E_{GABA} to negative potentials, resulting in more effective inhibition (Yamada et al., 2004; Dzhala et al., 2005; Sipilä et al., 2006; Dzhala et al., 2008; Rheims et al., 2008). The increase in inhibition has a significant anticonvulsant effect that is synergistic with anticonvulsants such as barbiturates that prolong the open probability of the GABA_A receptor mediated chloride channels (Twyman et al., 1989; Dzhala et al., 2005; Dzhala et al., 2008).

Several recent reports regarding the experimental treatment of neonatal seizures have reported conflicting results (Table 1). For example, if administered soon after the onset of seizures, phenobarbital is relatively more effective (Quilichini et al., 2003) and bumetanide is less effective (Kilb et al., 2007) as an anticonvulsant. In contrast, experiments in which drugs are administered after many seizures demonstrate reduced phenobarbital efficacy and increased efficacy of drugs such as bumetanide that block NKCC1-mediated shifts in E_{GABA} (Dzhala et al., 2005; Dzhala et al., 2008; Mazarati et al., 2009). Here we consider the possibility that activity-dependent, NKCC1-dependent changes in E_{GABA} help determine the time course of neonatal seizures. This hypothesis could explain the substantial variations in the efficacy of GABAergic anticonvulsants in the experimental settings described in Table 1. This hypothesis is also of considerable clinical importance, because it provides an additional impetus for immediate and aggressive treatment of neonatal seizures – the more seizures that occur, the more E_{GABA} will shift, and the lower the probability that the seizures will respond to available anticonvulsants such as phenobarbital, particularly during the crescendo phase of neonatal seizures (Painter et al., 1999). A corollary of this hypothesis is that by blocking NKCC1, bumetanide should prevent or reduce the seizure-induced shift in E_{GABA}, potentially ameliorating the crescendo pattern of neonatal seizures. Finally, enhancement of the efficacy of GABAergic anticonvulsants by bumetanide should increase with the duration of the prior seizure activity. These hypotheses are tested in whole hippocampal preparations from neonatal rats and CLM-1 mice.

Materials and Methods

Animals

All animal-use protocols conformed to the guidelines of the National Institutes of Health and the Massachusetts General Hospital Center for Comparative Medicine on the use of laboratory animals.

***In vitro* electrophysiology**

Intact hippocampal formations were prepared from neonatal postnatal day (P) 5–7 male and female CLM-1 mice pups, and P3–6 Sprague-Dawley rat male pups as described previously (Dzhala et al., 2008). Animals were anesthetized and decapitated. The brain was rapidly removed to oxygenated (95% O₂–5% CO₂) ice-cold (2–5° C) ACSF containing 126 mM NaCl, 3.5 mM KCl, 2 mM CaCl₂, 1.3 mM MgCl₂, 25 mM NaHCO₃, 1.2 mM NaH₂PO₄, and 11 mM glucose (pH 7.4). The hemispheres were separated and after removing the cerebellum, the frontal part of the neocortex and surrounding structures, the intact hippocampi were dissected from the septo-hippocampal complex. The hippocampi were incubated in oxygenated ACSF at room temperature (20–22° C) for 1–2 hours before use. For recordings, the hippocampi were placed into a conventional submerged chamber and continuously superfused with oxygenated ACSF at 32° C and at a flow rate 4 ml/min.

Extracellular field potentials were recorded in the intact hippocampal preparations *in vitro* using tungsten microelectrodes and low-noise multi-channel amplifier (band-pass 0.1 Hz – 10 kHz; x1000) (Suppl. Fig. 1). Microelectrodes made from coated tungsten wire of 50 μm diameter (California Fine Wire Company, Grover Beach, CA) were used for simultaneous recordings of population field activity in EEG band (0.1–100 Hz), ripple (100–200 Hz) and fast ripple oscillations (200–500 Hz), and multiple unit activity (MUA; 500 Hz high-pass filter). Root mean square (RMS) noise level with an electrode placed in the perfusion solution was typically 3–4 μV, while the amplitude of action potentials recorded from the pyramidal cell layer ranged from this noise level up to 60–80 μV. The signals were digitized using an analogue-to-digital converter (DigiData 1322A; Axon Instruments, USA). Sampling interval per signal was 100 μs (10 kHz). pCLAMP 9.2 (Axon Instruments, USA), Mini Analysis 5.6 (Synaptosoft, USA) and Origin 7.5 SR6 (Microcal Software, USA) programs were used for the acquisition and data analysis. Power spectrum analysis was performed after applying a Hamming window function. Power was calculated by integrating the RMS value of the signal in frequency bands from 1 to 1000 Hz.

Group measures are expressed as mean ± SEM; error bars also indicate SEM. Statistical tests of significance were assessed with Student's *t*, ANOVA, Chi-square, and Mann-Whitney tests as indicated in the results section. The level of significance was set at *p* < 0.05.

Clomeleon imaging and [Cl⁻]_i determination

Clomeleon is a fusion protein comprising the Cl⁻-sensitive yellow fluorescent protein (YFP) and the Cl⁻-insensitive cyan fluorescent protein (CFP). Transgenic CLM1 mice expressing Clomeleon were received from Duke University Medical Center (Durham, North Carolina) and housed at Massachusetts General Hospital Center for Comparative Medicine (Charlestown, MA). Intact hippocampi were prepared from neonatal (postnatal day (P) 5–7 days) mice as described previously (Dzhala et al., 2008). The hippocampi were incubated in oxygenated ACSF at room temperature (20–22° C) for at least 1 hr before use. For optical imaging and simultaneous extracellular field potential recordings, the hippocampus was placed into a conventional submerged chamber on a precision *x-y* stage mounted on the microscope and continuously superfused with oxygenated ACSF at 32° C and at a flow rate 4 ml/min. Two-photon Clomeleon imaging was performed on an Olympus Fluoview 1000MPE with pre-chirp excitation optics and a fast acousto-optical modulator mounted on an Olympus BX61WI upright microscope using an Olympus 20× water-immersed objective (XLUMPLFL 20×W; numerical aperture (NA): 0.95). A mode-locked titanium/sapphire laser (MaiTai; Spectra-Physics, Fremont, CA) generated two-photon fluorescence with 860 nm excitation. Emitted light passed through a dichroic mirror (460 nm cut-off) and was band-pass filtered through one of two emission filters 480 ± 15 nm (D480/30) for CFP and

535 ± 20 nM (D535/40) for YFP (FV10MP-MC/Y). Detectors containing two photomultiplier tubes were used. Image size (X-Y dimension) was 512×512 pixel or unit converted 634.662×634.662 μm. Clomeleon expressing neurons were typically sampled 20–200 micrometers below the surface of the intact hippocampus (Z dimension: 0–200 μm; step size: 2.00 μm). In ictal experiments, Clomeleon imaging was performed 1 minute after seizure termination to minimize pH-related changes in fluorescence (Xiong et al., 2000). Peak ictal changes in pH *in vitro* are approximately 0.02 pH units (Xiong et al., 2000), which would cause ≤ 2 mM change in our estimates of $[Cl^-]_i$ (Kuner and Augustine, 2000).

Quantitative measurements on 3D stacks were performed using ImageJ 1.40g software (National Institutes of Health, USA). The CFP and YFP images were opened and their respective background value was subtracted for the 3D volume. Median filtering was applied to all of the 3D planes. Cells were visually identified and a region of interest (ROI) was drawn around the cell bodies. The ratio of the YFP/CFP fluorescence intensity was measured for each identified cell. The $[Cl^-]_i$ was calculated from the following equation:

$$[Cl^-]_i = K'_D \frac{(R_{max} - R)}{(R - R_{min})} \quad (1)$$

where R is the measured YFP/CFP ratio, K'_D is the apparent dissociation constant of Clomeleon, R_{max} is the ratio when Clomeleon is not bound by Cl^- and R_{min} when it is completely quenched by F^- (Kuner and Augustine, 2000; Berglund et al., 2008). The constants K'_D , R_{max} and R_{min} were determined from the calibration of $[Cl^-]_i$ using solutions of known concentrations of Cl^- (20, 80 and 123 mM $[Cl^-]_o$). The K^+/H^+ ionophore nigericin (50 μM) and the Cl^-/OH^- antiporter tributyltin chloride (100 μM) were used to remove transmembrane H^+/OH^- and Cl^- gradients. Neurons that experienced a change in YFP/CFP intensity to each $[Cl^-]_o$ were used for the calibrations. The data points obtained with the different $[Cl^-]_o$ are described by rewriting equation 1 as the ratiometric function:

$$R = \frac{K'_D \cdot R_{max} + [Cl^-] \cdot R_{min}}{[Cl^-] + K'_D} \quad (2)$$

R_{max} and K'_D were free parameters, while R_{min} was determined by quenching Clomeleon with 123 mM F^- (Kuner and Augustine, 2000; Duebel et al., 2006). With single-cell resolution, R_{max} and K'_D were calculated for 47 individual neurons that were followed across all calibration conditions. The K'_D was 91 ± 5.43 mM, R_{max} was 1.026 and R_{min} was 0.268.

The mean of the logarithmic value of the $[Cl^-]_i$ was used in pseudocolor images, as the ion concentration follows a log-normal distribution. E_{Cl} was calculated using the Nernst equation setting the temperature variable at 33° C.

Two-photon fluorescence Ca^{2+} imaging

Both excitatory and inhibitory GABA responses are evident during status epilepticus in the intact hippocampus *in vitro*. The dense packing of cells in the pyramidal layer makes it difficult to directly measure these differential activity-dependent responses of individual neurons using extracellular recordings of multiple unit activity. Two-photon fluorescence imaging of bulk-loaded calcium dyes provides an optical proxy to single-cell electrophysiology with the inherent ability to multiplex. Simultaneous investigation of hundreds of neurons with single-cell resolution (Suppl. Fig. 1) makes it possible to

determine whether the responses to GABA indeed vary from cell to cell and, more importantly, how this response topology shifts after recurrent seizures. The high spatial resolution of this technique allowed us, in many instances, to follow the same cells across multiple conditions, e.g. in control vs. during and after spontaneous seizures, allowing us to use an individual cell as its own control.

We loaded hippocampal neurons with a calcium-sensitive dye under visual guidance through the two-photon microscope. A total of 0.8 mM Oregon Green 488 BAPTA-1 AM (OGB-1 AM) was dissolved in DMSO with 20% pluronic acid and mixed in ACSF containing SR-101, a red-fluorescent astrocyte-specific marker (all from Molecular Probes). A 2–3 μm patch pipette was filled with this solution and inserted into the intact hippocampus to a depth of 150–300 μm from the surface. The AM-dye, combined with SR-101, was pressure-ejected from the pipette (5–20 p.s.i. for 60–150s) under continuous visual guidance with multiphoton microscopy. OGB-1 AM is not fluorescent until fully hydrolyzed inside a cell—as a result the size of the micro-injection was estimated using the red-fluorescent signal from SR-101. Full loading of the OGB-1 AM dye took 0.5–1 h. After confirming loading, the pipette was withdrawn. Several hundred to thousands of cells were loaded from a single injection in a 300 micron diameter spherical region.

Time-lapsed two-photon calcium imaging was performed on the same microscope used for Clomeleon imaging. For continuous visual guidance during dye-loading, an Olympus 40X (numerical aperture, 0.80) was also used. OGB-loaded neurons were typically sampled 50–200 microns below the surface of the intact neonatal hippocampus.

Image Analysis

Time-lapsed images were analyzed in ImageJ (Wayne Rasband, NIH), Matlab (The MathWorks, Inc.) and Microsoft Office Excel (Microsoft Corporation) using custom-written software. Cells were automatically identified and time course data was extracted for each individual cell. On average, over 200 neurons could be imaged simultaneously in a given experiment. Astrocytes could be identified based on their uptake of SR-101. Cells were defined as responsive if there was a significant difference their baseline fluorescence and the fluorescence immediately after electrical stimulation. The peak response of the cell was defined as the maximum $\Delta F/F$ immediately after stimulation. Cells were considered to be inhibited by GABA if their response to stimulus during application of KYNA+CGP+SR 95531 (a potent GABA_A-R antagonist) significantly exceeded that under KYNA+CGP alone. In a subset of experiments, we were able to follow the same cells over the course of several hours to permit comparison across seizure and pharmacological conditions for the same cells. Before and after seizures, cells responses in three conditions (control, KYNA+CGP, and KYNA+CGP+SR 95531) were compared. If cells were inhibited by GABA, there would be a change in binary response probability (from inactive to active) or peak intensity (>15% increase) when comparing the KYNA+GGP+SR 95531 condition to KYNA only. In total we were able to analyze 468 cells in this manner. Of those that were inhibited by GABA ($n = 423$ neurons) we then determined the percentage that changed their polarity (“switched”)—i.e. how many cells that were initially inhibited by GABA shifted their response after spontaneous seizures. We did this by comparing the cellular response properties from before and after seizure (again using both binary response probability and peak $\Delta F/F$). Finally, since we had single-cell resolution across conditions, we correlated the probability of a single cell “switching” to the initial response characteristic (peak $\Delta F/F$) during control conditions before spontaneous seizures. We grouped cells based on their initial evoked response to electrical stimulus in control conditions and created a probability distribution based on the simple formula: number of cells that “switched”/total number of cells. We then determined whether there was a correlation between initial evoked response and the probability of switching.

Phospho-NKCC1 Western Blotting

Lysates were fractionated using 4–15% SDS/PAGE gradient gel electrophoresis (Bio-Rad, USA). Proteins were transferred to a poly(vinylidene difluoride) (PVDF) membrane (Bio-Rad, USA) at 100 V and 4°C for 2 h. The membrane was then blocked in 10% nonfat dried milk in PBS-T. Primary antibodies, including rabbit R5 anti-phospho NKCC1 (Flemmer et al., 2002) (gift of Dr. Biff Forbush, Yale University) and rabbit anti- β -tubulin (Cell Signaling, Inc.) were diluted, both at 1:500, in 5% milk in PBS-T and incubated with the membrane for 1 hour at room temperature. Blots were washed in PBS with 0.1% Tween 20 and probed with an HRP-conjugated anti-rabbit secondary antibody (Zymed) in 1% milk in PBS-T for 30 min at RT. The filter was then washed and chemiluminescence performed using ECL-Plus (Amersham Pharmacia), following standard protocols.

Drugs

Reagents were purchased from Sigma (Sigma-Aldrich Inc., USA) and Tocris (Tocris Cookson Inc., USA), prepared as stock solutions and stored before use as aliquots in tightly sealed vials at the manufacturers' recommended temperatures and conditions. Fluorescent probes were from Molecular Probes (Molecular Probes, Inc., USA).

Results

We used the intact hippocampal preparation (Khalilov et al., 1997) to preserve the neuronal network and avoid potential alterations in chloride transport and intracellular chloride concentration related to neuronal injury and axotomy (van den Pol et al., 1996; Nabekura et al., 2002) that may occur during slice preparation.

Distribution of resting $[Cl^-]_i$ and GABA action in the intact neonatal hippocampus

High resolution two-photon fluorescence chloride imaging was performed in the intact hippocampus *in vitro* of the neonatal (postnatal day (P) 5–7) transgenic mice CLM-1 expressing Clomeleon (Kuner and Augustine, 2000; Berglund et al., 2008; Glykys et al., 2009). The ratio of fluorescence resonance energy transfer (FRET)-dependent emission of the chloride-sensitive yellow fluorescent protein (YFP) to the chloride-insensitive cyan fluorescent protein (CFP) was used to measure intracellular chloride concentration ($[Cl^-]_i$) in CA3 pyramidal cells and interneurons (see Methods; Fig. 1a, b). Under control conditions, the resting $[Cl^-]_i$ in the individual neurons of the intact hippocampal preparations ($n = 10$ hippocampi) varied from 1 to 40 mM (Fig. 1) depending on cell size, type (*not shown*) and postnatal age (Tyzio et al., 2007; Glykys et al., 2009). Gaussian fits revealed a wide range of the resting intracellular chloride (Fig. 1b), suggesting heterogeneous populations of neurons, some with an equilibrium potentials for chloride (E_{Cl}) below the resting membrane potential (RMP), and others whose E_{Cl} is positive to RMP (Tyzio et al., 2003). This wide range of neuronal Cl^- is consistent with previously published data (Berglund et al., 2008; Tyzio et al., 2007; Glykys et al., 2009) and implies that both hyperpolarizing as well as depolarizing GABA_A receptor (GABA_A-R) mediated signaling occurs in large populations of developing neurons, via inwardly and outwardly directed Cl^- fluxes.

The net effect of GABA_A-R activation on the frequency of spontaneous action potentials was measured in intact hippocampi prepared from neonatal (P5–7) CLM-1 mice (Fig. 1 c–e). Non-invasive extracellular recordings of multiunit activity (MUA) were performed in the CA3 pyramidal cell layer (Suppl. Fig. 1). Bath application of the selective agonist of GABA_A-R isoguvacine (10 μ M for 1 min) transiently reduced spontaneous neuronal firing rate by 91.5 ± 3.1 % in 12 recordings from 6 intact hippocampi (Fig. 1 c–e), indicating that the net effect of GABA_A-R activation in the intact hippocampal network was inhibitory. In

contrast, in the neonatal hippocampal and neocortical slice preparations, a more uniformly depolarizing Cl^- equilibrium potential (Glykys et al., 2009) and a consequent excitatory action of GABA_A -R activation (Dzhala et al., 2005) leads to a net increase in spontaneous firing rates of neurons and an increased frequency of spontaneous population bursts in response to GABA_A -R agonists (Tyzio et al., 2007; Dzhala et al., 2008).

Progressive $[\text{Cl}^-]_i$ accumulation and change in the action of GABA during recurrent seizures

Positive (excitatory) shifts in the reversal potential for GABA_A receptor-mediated responses were observed in immature neurons after prolonged seizure activity (Khalilov et al., 2003). We considered the possibility that neuronal chloride accumulation and a consequent excitatory shift in GABA action occur and persist during recurrent seizure activity. Simultaneous high resolution two-photon fluorescence chloride imaging and extracellular field potential recordings were performed in intact hippocampi prepared from neonatal (P5–7) CLM-1 mice (Kuner and Augustine, 2000; Berglund et al., 2008). Persistent bath application of low- Mg^{2+} ACSF induced recurrent interictal and ictal-like (seizure) epileptiform discharges (Fig. 2a, for details, see (Dzhala et al., 2008)), which gradually increased in frequency (Quilichini et al., 2002; Quilichini et al., 2003; Dzhala et al., 2008) and power (Dzhala et al., 2008) (Fig. 2e – g; Fig. 5e, f). Starting from onset, the mean inter-seizure interval significantly decreased by 39 % from 515.4 ± 29.7 to 315.7 ± 35.6 sec ($n = 8$, $p = 0.0008$; Fig. 5e). Over a 1-hour period of low- Mg^{2+} ACSF application, the normalized mean power of recurrent ictal-like events increased by 61 ± 24 % ($p = 0.039$; Fig. 5f). These data are consistent with the hypothesis that neonatal seizures increase the probability of subsequent seizures.

The $[\text{Cl}^-]_i$ in CA3 pyramidal cells was measured between recurrent seizures as a function of the quantity (N) of preceding seizures (Fig. 2 a–d; Table 2). After 1–2 seizures, 35 % of CA3 neurons accumulated chloride more than 10 mM above the resting $[\text{Cl}^-]_i$. After 7–8 seizures, 71% of CA3 neurons accumulated chloride more than 10 mM above the resting $[\text{Cl}^-]_i$. These changes were of sufficient magnitude to shift the E_{Cl} above the predicted resting membrane potential, implying a shift in GABAergic signaling from inhibitory to excitatory. Depolarized values of E_{Cl} in a subpopulation of CA3 neurons persisted for a long time (at least 1–2 hours) after cessation of recurrent seizures by perfusion of control ACSF (*not shown*) and may contribute to the generation of subsequent spontaneous seizures (Khalilov et al., 2003; Nardou et al., 2009). Application of low- Mg^{2+} ACSF in the presence of the sodium channel blocker TTX (1 μM) did not alter intracellular chloride concentration ($n = 3$; *not shown*) suggesting that changes in $[\text{Cl}^-]_i$ were caused by seizure activity. Thus, recurrent seizures caused a progressive intracellular chloride accumulation as a function of the quantity of preceding seizures.

To test whether the ictal increase in $[\text{Cl}^-]_i$ altered the effect of GABA_A -R activation, we tested whether the action of the GABA_A -R agonist isoguvacine on neuronal activity (Fig. 1 c–e) is altered by seizure activity. We tested whether isoguvacine increased or decreased multiunit activity, which allowed us to separate the effects of alterations in E_{GABA} (Dzhala and Staley, 2003; Ben-Ari et al., 2007) from changes in GABA release (Hirsch et al., 1999) and postsynaptic GABA_A -R conductance (Naylor et al., 2005; Goodkin et al., 2008). If GABA-mediated excitation progressively increases during the time-course of spontaneous epileptiform activity, then the GABA_A -receptor agonist should increase the neuronal firing rate and the frequency of epileptiform discharges proportionally to the number and duration of preceding seizures. If on the other hand GABA_A -R function is inhibitory but limited by postsynaptic reductions in GABA conductance (Naylor et al., 2005; Goodkin et al., 2008), we would see a reduction but not a reversal in the inhibitory effects of exogenous GABA_A -R agonists. Finally if GABA effects were limited by presynaptic reduction in GABA release

(Hirsch et al., 1999), we would see no net change in the effects of exogenous GABA_A-R agonists.

Interictal and ictal-like epileptiform discharges were induced by persistent bath application of low-Mg²⁺ ACSF in intact hippocampi prepared from neonatal (P5–7) CLM-1 mice. Figure 3 illustrates the typical effects of isoguvacine (10 μM for 1 min) on MUA and epileptiform discharges. Application of isoguvacine after the first seizure, shortly after recovery from post-ictal depression, invariably reduced MUA frequency (n = 6). After 2–3 seizures, isoguvacine transiently increased the frequency of MUA, in association with a transient increase of the frequency of interictal epileptiform discharges (IEDs). The transient excitatory action of isoguvacine was followed by a suppression of interictal and multiple unit activity (Fig. 3 a–c), consistent with activity-dependent reduction in [Cl⁻]_i (Brumback and Staley, 2008). In 3 out of 6 experiments, application of isoguvacine failed to block interictal activity. After 4–6 recurrent seizures, isoguvacine transiently increased the frequency of MUA and IEDs and often induced ictal-like epileptiform discharges (6 out of 9 applications of isoguvacine). However, this does not exclude a coincidence of the effect of isoguvacine with recurrent seizure activity (*not shown*).

Thus, neonatal seizures alter polarity of the GABA_A-R mediated signaling and invert the net effect of GABA_A-R activation from inhibition to transient excitation. Positive shifts in E_{Cl} and corresponding changes in GABA action may contribute to facilitation of recurrent seizures and resistance of recurrent seizures to GABAergic anticonvulsants.

Efficacy of Phenobarbital depends on the quantity of seizure activity

The ictal shifts in [Cl⁻]_i and E_{GABA} can initiate a positive feedback cycle in neonatal seizures (Staley and Smith, 2001), and a depolarized value of E_{GABA} may contribute to the reduced efficacy of GABA-enhancing anticonvulsants (Dzhala et al., 2005; Dzhala et al., 2008). We therefore tested the effects of Phenobarbital on recurrent seizure activity as a function of the number of preceding seizures. Extracellular field potential recordings were performed in the CA3 pyramidal cell layer in the neonatal rat (postnatal day (P) 3–6) whole-hippocampal preparations *in vitro*. Bath application of low-Mg²⁺ ACSF induced recurrent ictal-like (seizure) epileptiform activity (Fig. 4a, d; for details, see (Dzhala et al., 2008)).

The anticonvulsant efficacy of Phenobarbital, measured in terms of reduction in the frequency and power of recurrent seizures, was evaluated as a function of the quantity (N) of preceding seizures (Fig. 4 b–e). A high concentration of phenobarbital (100 μM) was bath applied for 60 min. The mean frequency of seizures in the presence of phenobarbital after one preceding seizure (n = 8) was significantly lower than in control low-Mg²⁺ ACSF (Fig. 4d). After 7 preceding seizures, the mean frequency of recurrent seizures in presence of phenobarbital was 3.3 ± 0.6 seizures per hour (n = 7), not significantly different than control (p > 0.05; Fig. 4d). Application of Phenobarbital after one or two seizures abolished recurrent seizures in 4 out of 8 experiments (50 %; Fig. 4e). After 3 to 5 preceding seizures, phenobarbital abolished recurrent seizures in 2 out of 7 experiments (28.6 %), and after 6–8 seizures, in one out of 11 experiments (9 %). Phenobarbital applied after one seizure depressed the power of extracellular field potential activity by 81.8 ± 8.4 % (n = 8, p=0.0036) of preceding control power, but Phenobarbital applied after 7 preceding seizures decreased power by only 45 ± 15.3 % (n = 7, p=0.027) of preceding power.

Thus, neonatal seizures progressively reduce the anticonvulsant efficacy of Phenobarbital. The anticonvulsant efficacy of Phenobarbital was inversely proportional to the quantity of preceding seizures (Fig. 4).

NKCC1 co-transporter contributes to seizure-induced chloride accumulation and the facilitation of recurrent seizures

Immature neurons express high levels of the NKCC1 (Delpire, 2000; Wang et al., 2002; Dzhala et al., 2005) electroneutral co-transporter that imports Na^+ , K^+ and Cl^- . We therefore assessed the contribution of NKCC1 co-transporter to ictal $[\text{Cl}^-]_i$ accumulation by perfusing the NKCC1 antagonist bumetanide (10 μM) after the first or second seizure induced by continuous superfusion of low- Mg^{2+} ACSF in the intact hippocampus *in vitro* of the neonatal (P5–6) CLM-1 mice (Fig. 5; Table 2). Figure 5d illustrates the mean effects of recurrent seizures on intracellular chloride accumulation in control low- Mg^{2+} + ACSF (mean \pm s.e.; 187 cells from $n=4$ intact hippocampi) and in the presence of bumetanide (185 cells from $n=4$ hippocampi). Notably, bumetanide not only reduced the mean ictal increase in $[\text{Cl}^-]_i$ (Fig. 5 b–d; Table 2), but also reduced the fraction of cells that accumulated chloride more than 10 mM above baseline chloride level in control low- Mg^{2+} ACSF. In the presence of bumetanide, the fraction of cells that accumulated chloride after 7–8 recurrent seizures more than 10 mM above the baseline resting chloride level was 31% (vs 71% in control).

Additionally, bumetanide prevented the progressive increase in the power and frequency of recurrent seizures induced by low- Mg^{2+} ACSF (Fig. 5e, f; Suppl. Fig. 2, 3). Over a 1-hour period of simultaneous low- Mg^{2+} ACSF and bumetanide superfusion, the mean inter-seizure interval was not significantly different (495 ± 59 s vs 417.4 ± 33.3 sec; $n = 8$, $p = 0.36$; Fig. 5e). The mean power of ictal-like events was also not significantly different (105 ± 22 % of control, $p = 0.8$; Fig. 5f).

We tested also whether NKCC1 block prevented excitatory shift in the action of GABA induced by recurrent seizures (Fig. 3). Figure 6 illustrates the typical effects of isoguvacine (10 μM for 1 min) on MUA and epileptiform discharges in the presence of bumetanide. Application of isoguvacine after the first seizure ($N = 1$), shortly after recovery from post-ictal depression, transiently reduced MUA frequency by 87 ± 4 % (8 recordings in $n = 4$ hippocampi). Inhibitory action of isoguvacine persisted also after 2–3 as well as after 4–5 recurrent seizures (Fig. 6). After 2–3 seizures, isoguvacine application did not induce epileptiform discharges and transiently reduced the frequency of MUA by 83.5 ± 4 % (8 recordings in $n = 4$ hippocampi). After 4–6 recurrent seizures, isoguvacine transiently reduced the frequency of MUA by 74.6 ± 6.2 % (8 recordings in $n = 4$ hippocampi). In 1 out of 4 experiments, recurrent seizures ($N = 6$) were followed by persistent interictal-like epileptiform discharges. Application of isoguvacine transiently abolished these epileptiform discharges (*not shown*).

Thus the diuretic bumetanide prevented or reduced seizure-induced progressive $[\text{Cl}^-]_i$ accumulation in large sub-populations of neurons (Fig. 5c; Table 2) as well as prevented changes in the action of GABA (Fig. 6), and reduced seizure-dependent facilitation of recurrent seizures (Fig. 5 e and f; Suppl. Fig. 2, 3).

Potential mechanism of increased NKCC1 activity during recurrent seizures

NKCC1 is an electro-neutral bi-directional transporter that can carry out net Na^+ , K^+ and 2Cl^- ion influx or efflux, depending on the concentration gradients of the transported ions (Payne, 1997; Gamba, 2005; Brumback and Staley, 2008). The activation of NKCC1 requires phosphorylation of Thr-212 and Thr-217 in the cytoplasmic amino terminus (Flemmer et al., 2002; Darman and Forbush, 2002; Payne et al., 2003). We monitored the phosphorylation of NKCC1 at these sites with anti-R5, an antibody that specifically recognizes phosphorylation of Thr-212 and Thr-217 *in vitro* and *in vivo* (Flemmer et al., 2002; Darman and Forbush, 2002; Gimenez and Forbush, 2003). Western blotting detected phospho-NKCC1 in both

control and seizure conditions (Suppl. Fig. 4). These findings indicate that NKCC1 is present, phosphorylated, and presumably active in hippocampi from neonatal mice with recurrent seizures, but they do not provide evidence that increased seizure activity is associated with increased phosphorylation of NKCC1 at its known regulatory sites.

Recurrent seizures in neonatal and adult cortical structures have long been known to cause acute, activity-dependent alterations in neuronal ion concentrations (Moody et al., 1974; Heinemann et al., 1977; Khalilov et al., 1999b; Xiong and Stringer, 2000). In the intact neonatal hippocampal formation, recurrent ictal-like epileptiform discharges increase extracellular concentration of K^+ ($[K^+]_o$) to 12.5 mM (Khalilov et al., 1999b). Ictal accumulation of extracellular potassium will increase the $[Cl^-]_i$ at which NKCC1 transport reaches equilibrium (Brumback and Staley, 2008). We therefore assessed the contribution of NKCC1-mediated co-transport to intracellular chloride accumulation as a function of extracellular concentration of K^+ (Fig. 7 a–e). In the presence of sodium channel blocker TTX (1 μ M), increasing $[K^+]_o$ from 3.5 mM (control) to 8.5 mM resulted in a corresponding increase in $[Cl^-]_i$ from 19.9 ± 0.8 mM to 26.9 ± 1.2 mM ($p < 0.05$ vs baseline $[Cl^-]_i$, ANOVA followed by Tukey's means comparison test; $n = 138$ cells in 4 hippocampi; Fig. 7e). Increasing $[K^+]_o$ to 13.5 mM increased $[Cl^-]_i$ to 45.6 ± 2 mM ($p < 0.05$). In the presence of bumetanide (10 μ M), increasing $[K^+]_o$ from 3.5 mM to 8.5 mM resulted in a corresponding increase in $[Cl^-]_i$ from 17.4 ± 0.9 mM to 18.4 ± 1 mM; $p = 0.43$, $n = 132$ cells in 4 hippocampi (Fig. 7e). Increasing $[K^+]_o$ to 13.5 mM increased $[Cl^-]_i$ to 21.8 ± 1 mM ($p = 0.02$). However, this increase in the presence of bumetanide was 23.8 mM lower than in control conditions (21.8 ± 1 mM vs. 45.6 ± 2 mM; $p < 0.05$; Fig. 7e). Thus, seizure-induced $[K^+]_o$ elevation is sufficient to increase $[Cl^-]_i$ accumulation via NKCC1 co-transport resulting in alterations of E_{GABA} during recurrent seizures (Fig. 2, 3, 5, 6).

NMDA receptor, NKCC1 activity and inverted action of GABA

The NKCC1 phosphorylation data and $[K^+]_o$ data suggest that at least some aspects of ictal changes in $[Cl^-]_i$ may be independent of calcium-dependent signal transduction mechanisms. On the other hand, epileptogenic transformation of the intact hippocampal neuronal network required voltage-dependent activation of NMDA-Rs and long-term alterations in GABAergic synapses, which became excitatory because of a positive shift in the chloride reversal potential (Khalilov et al., 2003). We therefore determined the contribution of NMDA-R to seizure-induced changes in the net effect of GABA_A receptor activation and corresponding alterations of recurrent seizures (Fig. 2, 3, 5). Since seizures are NMDA-R dependent in the low- Mg^{2+} model, we used the kainic acid model of epileptiform activities in the intact neonatal hippocampus *in vitro* of the neonatal (P5–6) mice (Prince et al., 1973; Fisher et al., 1976; Khalilov et al., 1999b).

In control ACSF, transient application of kainic acid (1 μ M for 4–5 min) progressively increased the frequency of MUA and induced interictal and ictal-like epileptiform discharges followed by a post-ictal depression (8 recordings in $n = 4$ hippocampi; Fig. 8a). Repeated applications of kainic acid (5 applications at 15 min intervals) induced inter-ictal and ictal-like epileptiform discharges that progressively increased in amplitude and power (Fig. 8d). After five applications of kainic acid, spontaneous recurrent epileptiform discharges were generated in 3 out of 4 intact hippocampi. Brief applications of isoguvacine (10 μ M for 1 min) transiently increased the frequency of spontaneous epileptiform discharges by 225 ± 154 % ($p = 0.04$; 6 applications in $n = 3$ hippocampi; Fig. 8 a, e) suggesting seizure-induced changes in the action of GABA and contribution of the excitatory action of GABA to generation of spontaneous recurrent epileptiform discharges.

We determined whether the non-competitive NMDA-R antagonist MK801 prevented seizure-induced changes in the net effect of GABA_A-R activation from inhibition to

excitation assayed by the frequency of spontaneous action potentials and/or interictal epileptiform discharges (Fig. 8 b, e). In the presence of MK801 (20 μ M), transient applications of kainic acid induced interictal and ictal-like epileptiform discharges that progressively decreased in amplitude and power (6 recordings in $n = 3$ hippocampi; Fig. 8d). Persistent perfusion of MK801 did not prevent generation of spontaneous epileptiform discharges induced by repeated applications of kainic acid. Brief applications of isoguvacine (10 μ M for 1 min) in the presence of MK 801 transiently increased the frequency of spontaneous epileptiform discharges by $368 \pm 129\%$ ($p = 0.015$; 6 applications in $n = 3$ hippocampi; Fig. 8 b, e) before depressing them. These effects are similar to what was seen in control conditions (Fig. 2), suggesting that NMDA-R did not contribute to seizure-induced chloride accumulation and the corresponding changes in the action of GABA.

As in control conditions, the NKCC1 antagonist bumetanide (10 μ M) prevented the seizure-induced excitatory shift in the action of GABA ($n = 3$; Fig. 8 c, e) in the presence of MK801 (20 μ M). In the presence of MK 801 and bumetanide, repeated applications of kainic acid (5 applications for 5 min each; 15 min intervals) induced interictal and ictal-like epileptiform discharges that progressively decreased in power and amplitude (Fig. 8 c, d). Spontaneous epileptiform discharges after five applications of kainic acid were recorded in one out of three experiments (33.3 %). Brief applications of isoguvacine (10 μ M for 1 min) abolished spontaneous epileptiform discharges (two recordings in $n = 1$ hippocampus) and/or reduced the frequency of MUA (six recordings in $n = 3$ hippocampi). Thus seizure-induced NKCC1-dependent chloride accumulation and the excitatory shift in the action of GABA was NMDA-receptor independent.

Long-term pro-convulsive effect of GABA_A-receptor antagonist

The pro-convulsive effect of complete blockade of GABA_A-R indicates that at P4–6, GABA_A receptors subserve a significant inhibitory function (Khalilov et al., 1999a; Wells et al., 2000). In those studies, the GABA_A-R antagonists bicuculline and picrotoxin induced glutamate-receptor mediated interictal and ictal-like activities in the intact hippocampus. We determined the long-term effect of GABA_A-R antagonist SR 95531 (Gabazine) on spontaneous neuronal activity. We performed non-invasive extracellular field potential recordings of synchronous population activity and multiple unit activity (MUA) in the CA3 pyramidal cell layer in the intact hippocampal preparations from P4–6 rats (Suppl. Fig. 1). In control ACSF, bath application of SR 95531 (10 μ M for 3–4 min) progressively increased the frequency of MUA by $44 \pm 13.2\%$ from 13.5 ± 1.7 to 19.3 ± 2.8 spikes s^{-1} ($p = 0.004$; $n = 14$ recordings in 8 hippocampi) (*not shown*) and rapidly, within 2–3 minutes, induced interictal and ictal-like epileptiform discharges followed by a post-ictal depression with reduced neuronal activity (Fig. 9a). After removal of the drug and shortly after post-ictal depression, recurrent interictal and tonic-clonic epileptiform discharges occurred in all intact hippocampi for an extended period of 30–60 min (mean, 42.8 ± 2.8 min for $n = 16$ hippocampi at P4–5). Spontaneous epileptiform discharges, in some experiments, persisted for several hours in drug-free ACSF (*not shown*), suggesting that their persistence was not related to residual antagonist but rather due to activity-dependent long-term changes in synaptic plasticity (Bains et al., 1999; Schneiderman et al., 1994; Abegg et al., 2004; Arnold et al., 2005). We considered the possibility that spontaneous epileptiform discharges induced by GABA_A-R blockade were as effective as low Mg^{2+} -induced activity in inducing the shift in neuronal $[Cl^-]_i$ and the net action of GABA_A-R activation.

Recurrent seizures cause progressive NKCC1-dependent change in the action of GABA

In control conditions, brief bath application of isoguvacine (10 μ M for 1 min) transiently reduced the frequency of MUA by $63.4 \pm 5.7\%$ ($p = 0.0009$; $n=6$) (Fig. 9 b, d, e). Spontaneous interictal and ictal-like epileptiform discharges were then induced by transient

application of the GABA_A-R antagonist SR 95531 (10 μM for 3 min; Fig. 9a). 30 min after onset of spontaneous epileptiform discharges, bath application of isoguvacine transiently increased the frequency of multiple unit activity frequency by $60.3 \pm 22.1\%$ ($p = 0.007$; $n = 6$), in association with a transient increase of the frequency of interictal epileptiform discharges (IED) (Fig. 9b, d). Subsequently, MUA frequency decreased, consistent with activity-dependent reduction in $[Cl^-]_i$ (Brumback and Staley, 2008). 60–70 min after onset of spontaneous seizures, isoguvacine transiently increased the frequency of MUA by $59.3 \pm 22\%$ ($p = 0.015$), in association with transiently induced IEDs, followed by a decrease as seen at 30 minutes. The biphasic action of isoguvacine persisted at least for 1–2 hours after termination of spontaneous epileptiform discharges.

In the presence of bumetanide, application of isoguvacine (10 μM for 1 min) transiently reduced the frequency of MUA by $82.7 \pm 4.2\%$ ($p = 0.0004$; $n = 6$; Fig. 9c, d, e). 30 min after onset of spontaneous epileptiform discharges induced by SR 95531, isoguvacine reduced MUA frequency by $44.3 \pm 14.4\%$ ($p = 0.015$; $n=6$) and did not induce epileptiform discharges or increase the frequency of epileptiform discharges (Fig. 9c, d). 60–70 min after onset of spontaneous epileptiform discharges, isoguvacine invariably diminished MUA frequency by $50.7 \pm 16.3\%$ ($p = 0.002$; $n=6$). Thus the diuretic bumetanide prevents or reduces seizure-induced changes in the action of GABA during spontaneous seizures and after termination of seizures. In summary, while these data do not exclude pre- or postsynaptic alterations in GABA conductance, they demonstrate a clear reversal of the effect of GABA_A-R activation that is NKCC1-dependent, and independent of the mechanism of seizure induction. These data support the idea that NKCC1 activity underlies the post-ictal increase in $[Cl^-]_i$ (Fig. 2, 5) and the excitatory effects of GABA.

NKCC1-dependent changes contribute to the time course of spontaneous seizures

To determine whether the seizure-induced, NKCC1-dependent changes in GABA_A-R function contribute to the increased probability of subsequent seizures (Dzhala and Staley, 2003; Dzhala et al., 2005; Dzhala et al., 2008; Khazipov et al., 2004), we assessed the effects of NKCC1 co-transporter blocker bumetanide on the time course of spontaneous seizures assayed by the quantity, duration and power of spontaneous epileptiform activity in the P3–5 intact hippocampal preparations (Suppl. Fig. 5 a–e). In control ACSF, brief application of SR 95531 (10 μM) induced spontaneous seizures in 16 out of 18 preparations. The duration of this status epilepticus was 41.7 ± 2.5 min ($n = 16$). In the presence of bumetanide, similarly brief application of SR 95531 induced a shorter period of spontaneous interictal and ictal-like discharges (31.3 ± 2.2 min, $p = 0.004$; Suppl. Fig. 5c) in 10 out of 15 preparations. The number of spontaneous ictal-like episodes induced by GABA_A-R block was not significantly different: 2.1 ± 0.3 seizures in SR 95531 and 1.8 ± 0.3 seizures in the presence of SR 95531 + bumetanide ($p = 0.7$; Suppl. Fig. 5c). We also assessed the power of SR 95531-induced epileptiform activity in control ACSF and in the presence of bumetanide (Suppl. Fig. 5d and e). The effect of bumetanide on EEG power was relatively low shortly after washout of GABA_A-R antagonists (~10%) but gradually increased to ~45% by the end of the seizure activity induced by transient exposure to SR 95531. While these data support a progressive, seizure-induced increase in $[Cl^-]_i$ and excitatory shift in GABA_A-R function, the alternative possibility was that SR 95531 was incompletely washed out early, in which case the impact of bumetanide on NKCC1 would initially be minimized due to reduced GABA_A receptor-mediated chloride conductance. This was unlikely because we had already seen a stable impact of GABA_A-R agonist application (Fig. 9d) at different time points after washout of SR 95531 during and after spontaneous seizures. We conclude that neonatal seizures increase the probability of recurrent neonatal seizures via NKCC1-dependent chloride accumulation and consequent alteration in GABA actions.

Neonatal seizures change the polarity of synaptic GABA_A responses

To further characterize the mechanisms of seizure-induced alterations in $[Cl^-]_i$, GABA actions and seizure activity, we assessed the effects of *endogenously* released GABA on neuronal firing rate and epileptiform activity and as a function of the number of seizures.

The net effect of GABA_A-R activation may be inhibitory even when E_{GABA} is positive to resting membrane potential. Large GABA_A-R mediated anion conductance effectively reduces the input membrane resistance and thereby shunts excitatory glutamatergic inputs, resulting in suppression of neuronal activity (Qian and Sejnowski, 1990; Staley and Mody, 1992; Khalilov et al., 1999a). We determined whether the inhibitory operation of GABA_A-R in the intact hippocampal network was mediated by synaptic inhibitory mechanism and whether neonatal seizures alter this inhibition. Pharmacological protocols were used to determine the contributions of intrinsic and synaptic activities to the generation of neuronal discharges and estimate the degree to which endogenous synaptic activity altered spontaneous neuronal firing rate in population of neurons (Dzhala and Staley, 2003; Cohen and Miles, 2000). In control conditions, bath application of the AMPA and NMDA receptor antagonists kynurenic acid (KYNA; 2 mM) and metabotropic GABA_B receptor antagonist CGP 55845 (CGP; 1 μ M) significantly reduced neuronal firing rate by 32.5%, from 12.3 ± 1.3 to 8.3 ± 0.8 spikes s^{-1} ($n = 14$; $p = 0.0002$, paired t-Test; Fig. 10a). Subsequent application of the selective, competitive GABA_A-R antagonist SR 95531 (10 μ M), in the presence of KYNA and CGP 55845, increased neuronal firing rate in 10 of 14 recordings, and did not significantly change neuronal firing rate in the remaining 4 recordings (Fig. 10a). The average mean frequency of neuronal discharges under these conditions increased by 21% from 8.3 ± 0.8 to 10.04 ± 0.9 spikes s^{-1} ($p = 0.009$). These findings are consistent with the pro-convulsive effect of GABA_A-R antagonists in the intact hippocampal preparation (Khalilov et al., 1999a) and indicate a net inhibitory action of endogenously released GABA in the intact CA3 hippocampal network at this early postnatal age (P3–5).

To determine whether the action of endogenously released GABA is altered by prior seizure activity, we measured the impact of GABA_A-R block on the rate of spontaneous action potentials as a function of the number of preceding seizures in the CA3 pyramidal cell layer of the intact neonatal (P3–5) hippocampus. Spontaneous seizures were induced by brief application of SR 95531 (10 μ M for 3–4 min). 30–40 min after onset of spontaneous epileptiform discharges, bath application of KYNA (2 mM for 10 min) in combination with CGP 55845 (1 μ M) abolished epileptiform discharges and reduced the neuronal firing rate by 50%, from 10.3 ± 2.3 to 5.3 ± 1.8 spikes s^{-1} ($n=14$, $p=0.002$; Fig. 10b). Subsequent application of the GABA_A-R antagonist SR 95531, in the presence of KYNA and CGP 55845, induced three types of responses on MUA frequency: (i) significantly increased MUA frequency in 3 out of total 14 recordings; (ii) unchanged MUA frequency in 6 recordings, and (iii) significantly decreased MUA frequency in the remaining 5 recordings (Fig. 10b). The absence of an effect of SR 95531 on action potential frequency in the majority of recordings indicates that the net effect of GABA is no longer inhibitory after neonatal seizures. We also assessed the effect of endogenous GABA on neuronal firing rates as a function of the number of spontaneous seizures (Fig. 10c). We found a linear correlation between the number of spontaneous seizures and the action of GABA on neuronal firing rates. After 1–2 spontaneous seizures, the GABA_A-R antagonist SR 95531, when AMPA and NMDA receptors were blocked, did not significantly change the neuronal firing rate (112 ± 9.9 %; $p = 0.38$). After 3–4 spontaneous seizures SR 95531 diminished neuronal firing rate to 76 ± 11 % ($p = 0.017$), indicating that endogenous GABA was excitatory in a large population of neurons. Thus, spontaneous epileptiform discharges progressively reduce the rate of GABA_A-R mediated inhibition. This could be due to a number of factors including long-term potentiation of glutamatergic synapses between pyramidal cells induced by epileptiform activity (Ben-Ari and Gho, 1988; Bains et al., 1999), as evidenced by the

increased impact of KYNA on MUA during status epilepticus. However, glutamatergic mechanisms do not explain the alterations in MUA observed in the presence of KYNA. The loss of inhibitory effect of endogenously released GABA could arise from: (i) a positive shift in the chloride equilibrium potential in a large population of cells (Khalilov et al., 2003); (ii) a presynaptic reduction in GABA release (Hirsch et al., 1999); (iii) a reduction in the postsynaptic GABA_A conductance (Naylor et al., 2005). However, other than a long-term shift in E_{GABA} , none of these effects explain the post-ictal reduction in MUA frequency when GABA_A-Rs were blocked.

Cell specific actions of GABA on intracellular Ca²⁺ influx

The heterogeneity of neuronal $[Cl^-]_i$ (Fig. 1) and the post-ictal effects of endogenously released GABA in the preceding experiments raise the possibility that subpopulations of neurons may have distinct responses to GABA, either excitatory or inhibitory, and the MUA assay was measuring the network-wide average of those distinct responses. To analyze the response to GABA at the level of individual neurons, the action of GABA was assayed by changes in intracellular calcium (Stosiek et al., 2003). Large populations of CA3 neurons in the intact neonatal (P4–5) hippocampus were loaded with the calcium indicator dye Oregon Green BAPTA-1 AM (OGB) (Suppl. Fig. 1). Synchronous postsynaptic field potential responses and intracellular Ca²⁺ signals were induced by electrical stimulation in the *stratum radiatum* of CA3 area (Fig. 10d and e).

Under control conditions, electrical stimulation induced field excitatory postsynaptic potential (fEPSP) and synchronous Ca²⁺ transients in hundreds of CA3 neurons (Fig. 10d). On average, excitatory cellular responses (transient increases in $[Ca^{2+}]_i$ measured as $\Delta F/F$) were detected in $62.2 \pm 12.0\%$ of neurons (383 out of 616 cells; n values of 3 recordings) with an average $\Delta F/F$ of $6.8 \pm 0.1\%$ (Fig. 10f and g). We determined the degree to which synaptic excitation and inhibition contribute to these responses. Bath application of KYNA (2 mM), in combination with CGP 55845 (1 μ M), depressed the evoked field EPSPs and intracellular Ca²⁺ signals. Under these conditions, increases in $[Ca^{2+}]_i$ in response to electrical stimulation were detected in only 14.5% of neurons (91 out of 624 cells). In those cells that show increased in $[Ca^{2+}]_i$ the average peak signal intensity was a $\Delta F/F$ of $4.3 \pm 0.2\%$. Subsequent application of the GABA_A-R antagonist SR 95531 (10 μ M), in the presence of KYNA and CGP 55845, elicited an increase in the response to electrical stimulation measured by intracellular Ca²⁺ signals. Under these conditions, fluorescence calcium imaging revealed that both the percentage of responding cells ($73.5 \pm 12.0\%$) and the response amplitude ($\Delta F/F = 14.5 \pm 0.4\%$) were significantly higher than under the previous conditions ($p < 0.01$, Anova with post-hoc correction, Fig. 10f and g). These evoked increases in calcium in the presence of glutamate and GABA antagonists were presumably due to direct electrical stimulation of dendrites. After washing out of drugs, transient application of SR 95531 (10 μ M for 5 min) induced sustained ictal-like epileptiform activity followed by recurrent interictal and ictal-like epileptiform discharges. Under these conditions, 30–40min after onset of spontaneous seizures, electrical stimulation induced epileptiform discharges and corresponding Ca²⁺ signals in 99.4% of all cells (Fig. 10 e – g; 820 out of 825 cells; n values of 3 recordings). These responses were, on average, significantly amplified compared to control ($\Delta F/F = 27.4 \pm 0.6\%$, $p < 0.01$ ANOVA with post-hoc). In line with previous data, bath application of KYNA (2 mM) and CGP 55845 (1 μ M) abolished spontaneous and evoked epileptiform discharges and significantly decreased the percentage of responding cells (34.2%) and the corresponding response amplitude ($\Delta F/F = 11.7 \pm 0.5\%$; Fig. 10f and g). Subsequent application of SR 95531 (10 μ M), in the presence of KYNA and CGP 55845, failed to increase either cellular response probability (42.2%, 436 out of 1032 cells) or response amplitude ($\Delta F/F = 12.4 \pm 0.5\%$, 436 cells), indicating altered synaptic operation of the GABA_A receptors. This is in contrast to the response

elicited in control conditions, before seizure activity, in which block of GABA_A-R caused a dramatic rise of cellular response probability and $\Delta F/F$. Our data strongly suggest that neonatal seizures reduce the net inhibitory effect of endogenously released GABA.

The results described above do not differentiate whether GABA effects are homogeneously reduced after seizures, as could occur from either a shift in E_{GABA} or a reduction in the postsynaptic GABA conductance response, or whether GABA became excitatory in only a subpopulation of neurons. We therefore co-registered our images from the control and after seizure activity datasets, and automatically detected those cells that were clearly identifiable under both conditions. We then developed a simple measure to determine whether any of those cells “switched” from being inhibited by GABA in control conditions to being non-inhibited or excited by GABA post-ictally (Fig. 10h). We determined in which cells the stimulus-induced calcium transient was increased after GABA_A-R blockade under control conditions, and then, after spontaneous seizures, measured the fraction of those cells that still had an increase in stimulus-induced calcium transient after GABA_A-R blockade. We found that cellular responses were not uniform — not all cells had a loss of GABA-mediated inhibition after spontaneous seizures. Blockade of GABA_A-R under these conditions still enhanced the Ca^{2+} signal in 224 out of 423 cells ($p < 0.001$, Mann-Whitney Test), indicating that these cells were still inhibited by endogenously released GABA. The remaining 199 cells (~43%) switched post-ictally from being inhibited by endogenously released GABA to being excited or not inhibited by GABA (Chi-Square Test, 3 (inhibitory, neutral, excitatory) \times 2 (before seizures, after seizures), $p < 0.001$). Cells in this category demonstrated after block of GABA_A-Rs, either no stimulus-induced change in the calcium transients (157 cells, ~34%, $p > 0.05$, Mann-Whitney Test) or significantly reduced calcium transients (42 cells, ~9%, $p < 0.05$, Mann-Whitney Test). Thus after spontaneous seizure activity nearly half of all neurons undergo a transformation that causes them to lose their inhibitory response or switch their inhibitory response to endogenous GABA from inhibition to excitation.

Discussion

Our results demonstrate that NKCC1 activity strongly contributes to the intracellular chloride accumulation induced by recurrent seizures (Fig. 2, 5; Table 2). Activity-dependent shifts in $[K^+]_o$ (Moody et al., 1974; Heinemann et al., 1977), which alter the $[Cl^-]_i$ at which NKCC1 comes to equilibrium, are sufficient to cause these short-term changes in $[Cl^-]_i$ (Fig. 7), although other mechanisms may also be important. As a consequence, there is a sustained switch in the net effect of GABA_A-R activation from inhibition to excitation (Fig. 3,6,9). Shifts in E_{Cl} and GABA action contribute to facilitation of recurrent seizures and additional chloride accumulation. Under these conditions, recurrent seizures respond less well to GABAergic anticonvulsants, and better to the NKCC1 antagonist bumetanide, particularly when administered in combination with a positive allosteric GABA receptor modulator such as phenobarbital (Dzhala et al., 2008). Our data provide mechanistic insights into GABAergic excitation during neonatal seizures (Derchansky et al., 2008).

We previously demonstrated the anticonvulsant effects of bumetanide in a model of neonatal seizures *in vitro* (Dzhala et al., 2005; Dzhala et al., 2008). The reduced efficacy of bumetanide in other *in vitro* models of neonatal seizures (Kilb et al., 2007) likely reflects differences in the number of seizures prior to administration of bumetanide, because as predicted by the ictal, NKCC1-mediated increase in $[Cl^-]_i$ (Fig. 5) and as illustrated in Supplementary Figure 3, the anticonvulsant efficacy of bumetanide increases as a function of the number of seizures experienced by the preparation. Experimental data regarding the efficacy of GABA-enhancing anticonvulsants in neonatal seizures are controversial (Table 1). Some of this controversy may arise as a consequence of the heterogeneous values of E_{GABA} in the developing cortical networks (Figs. 1, 2, 5, 7), such that the net actions of

GABAergic agents in a particular slice preparation might be similarly varied. In addition, the ictal time course of changes in neuronal Cl^- are important experimental variables. *In vivo* models of neonatal seizures, primarily induced by GABA antagonists, demonstrate efficacy of GABAergic anticonvulsants administered before or coincident with convulsants (Velisek et al., 1995; Haugvicova et al., 1999; Isaev et al., 2007). As demonstrated in Figures 1–4, administration of phenobarbital prior to or just after the first seizure, when $[\text{Cl}^-]_i$ is relatively low and the net effect of GABA is still inhibitory, may prevent or reduce the positive feedback cycle of seizure-dependent disinhibition and subsequent disinhibition-induced seizures that limit the subsequent efficacy of GABAergic anticonvulsants.

Several mechanisms may be involved in activation of NKCC1 during recurrent seizure activity. NKCC1 activity is thought to be increased by phosphorylation (Darman and Forbush, 2002) and decreased by protein phosphatase one (PP1)-mediated dephosphorylation (Gagnon et al., 2007). NKCC1 phosphorylation corresponded to an increase in intracellular chloride in an *in vitro* model of ischemia (Pond et al., 2006). Our data (Suppl. Fig. 4) provide no indication that NKCC1 phosphorylation is increased by seizure activity, but do not address total NKCC1 protein levels nor membrane trafficking. However under conditions studied so far, activity-dependent increases in NKCC1-mediated Cl^- accumulation do not involve changes in NKCC1 maximum velocity or affinity for chloride, but rather changes in the trans-membrane ion gradients of the co-transported cations (Brumback and Staley, 2008), i.e. they do not involve alteration in total NKCC1 protein, NKCC1 membrane trafficking, or changes in NKCC1 phosphorylation (Suppl. Fig. 4).

$[\text{K}^+]_o$ increases during seizures (Prince et al., 1973; Fisher et al., 1976; Khalilov et al., 1999b), and elevated $[\text{K}^+]_o$ markedly alters the driving force for trans-membrane Cl^- co-transport (Thompson and Gahwiler, 1989; Staley and Proctor, 1999; Blaesse et al., 2009). This shift in free energy would be expected to lead to a corresponding increase in the $[\text{Cl}^-]_i$ at which NKCC1 reached equilibrium (Brumback and Staley, 2008) and would thus drive Cl^- influx via NKCC1 (Sun and Murali, 1998). Our experiments with increased $[\text{K}^+]_o$ strongly support this mechanism (Fig. 7), but do not exclude the possibility of additional mechanisms of modulation of NKCC1 and chloride accumulation.

Finally, paroxysmal depolarizing shifts in the membrane potential during seizures will induce Cl^- accumulation through open GABA_A -R; this phenomenon has been frequently exploited experimentally to load neurons with Cl^- (Staley and Proctor, 1999; Brumback and Staley, 2008). Such a mechanism may contribute to the small NKCC1-independent ictal increase in $[\text{Cl}^-]_i$ (Fig. 5B).

All DIC patch clampers select neurons to patch based on visual criteria related to cell turgor. Given the strong relationship between the activities of cation-chloride co-transporters and cell volume (Kahle et al., 2008), turgor is likely to be strongly correlated with neuronal chloride concentration. Patchable cells represent a very small subset of all neurons imaged with Clomeleon. Our results using Clomeleon extend the spectrum of actions of GABA during postnatal development (Ben-Ari et al., 2007) by demonstrating the wide range of $[\text{Cl}^-]_i$ and GABA effects in individual neurons in the developing hippocampus. Our data also underscore the importance of the history of activity of the preparation on neuronal $[\text{Cl}^-]_i$ and the consequent effects of GABA_A receptor activation. Our findings are consistent with prior observations of shifts in E_{GABA} as a consequence of trains of action potentials (Woodin et al., 2003; Brumback and Staley, 2008), seizures (Khalilov et al., 2003), trauma (van den Pol et al., 1996; Nabekura et al., 2002), and hypoxia (Pond et al., 2006). These long-term, experience dependent shifts in E_{GABA} may explain the incongruent results that have been obtained in developing preparations (Table 1).

The opposite effects of the GABA_A-R activation in the intact hippocampal preparations vs. the hippocampal slices probably arise from acute traumatic neuronal damage during slicing that may cause an increase in intracellular Cl⁻ concentration and consequent inversion of GABA action (van den Pol et al., 1996; Nabekura et al., 2002). Our results support reports of a predominantly inhibitory hyperpolarizing effect of GABA_A receptors in the neonatal hippocampus *in vivo* (Isaev et al., 2007). Additionally, perinatal hippocampal slice studies of the effects of GABA_A-R activation on [Ca²⁺]_i in CA3 neurons estimate 50% of P5 neurons are not excited by GABA (Tyzio et al., 2006), in agreement with Figure 10.

The biphasic effects of the GABA_A-R agonist isoguvacine on network action potential frequency (Figs. 3, 8, 9) likely represents activity-dependent shift in E_{GABA}. When NKCC1 is active and E_{GABA} is positive to membrane potential, low initial concentrations of isoguvacine activate GABA_A receptors and depolarize neurons. Subsequently, GABA channels are opened so persistently that the high fluxes of chloride overwhelm NKCC1-mediated chloride transport (Dzhala and Staley, 2003; Brumback and Staley, 2008). The clinical correlate of this experimental finding is that very high concentrations of GABAergic anticonvulsants are effective treatments of neonatal seizures (Mizrahi and Kellaway, 1987), presumably via the same mechanism – overwhelming NKCC1-mediated Cl⁻ transport with chloride flux through persistently opened GABA_A-R operated ion channels. The consequent passive trans-membrane distribution of Cl⁻, together with the low membrane resistivity induced by persistent GABA_A-R activation permits effective shunting inhibition. The potential disadvantage of using high doses of GABAergic anticonvulsants to treat neonatal seizures is the level of GABA-mediated suppression of brainstem and spinal circuits that have already undergone the developmental switch from NKCC1-mediated neuronal Cl⁻ import to KCC2-mediated neuronal Cl⁻ export (Stein et al., 2004) (Glykys et al., 2009), as well as increased anticonvulsant-induced neuronal apoptosis (Ikonomidou, 2009). Although there are also potentially deleterious effects of NKCC1 inhibition (Ge et al., 2006; Cancedda et al., 2007; Wang et al., 2008), these are evident after much more prolonged inhibition than would be necessary to control most neonatal seizures (Painter et al., 1999).

Recurrent seizures in neonatal and adult cortical structures cause activity-dependent alterations in ion concentrations (Fisher et al., 1976; Cohen et al., 2002; Khalilov et al., 2003; Li et al., 2008; Galanopoulou, 2008). Here we demonstrate that changes in ion transport persist beyond the end of seizure activity to contribute to recurrence of seizures. These findings are of particular interest in understanding the natural history of neonatal seizures. Prospective EEG studies in which clinically silent electrographic seizures were untreated (Connell et al., 1989) support the clinical impression that seizures due to brain injury begin hours after the insult and continue for approximately 72 hours (Volpe, 2001). The NKCC1-mediated delayed increase in neuronal chloride concentration following hypoxic/aglycemic injury (Pond et al., 2006) together with the observation that increases in NKCC1 transcription persist for 72 hours after injury *in vivo* (Dai et al., 2005) support the hypothesis that increases in NKCC1 activity and consequent compromise of GABA-mediated inhibition contribute significantly to the time course of neonatal seizures following hypoxic-ischemic brain injury (Cowan et al., 2003; Tekgul et al., 2006). Induction of NKCC1 by hypoxic injury may explain why rapid EEG diagnosis and treatment of neonatal seizures has not had a bigger impact on the efficacy of phenobarbital therapy (Painter et al., 1999; Bartha et al., 2007), as might be predicted from Figure 2. By the time the first seizure has occurred, NKCC1 activity may already be increased due to the prior hypoxia so that early treatment with phenobarbital is still too late to rescue GABA_A-R mediated inhibition. An open question is whether prophylactic treatment with bumetanide would reduce the incidence or severity of neonatal seizures.

Supplementary Material

Refer to Web version on PubMed Central for supplementary material.

Acknowledgments

This work was supported by the United States of America National Institutes of Health and National Institute of Neurological Disorders and Stroke grant NS 40109-06 to K.S., and in part by NIH grant EB000768 to B.B., NS580752 to K.K., AES grant to J.G. and Hearst foundation grant to V.D.

Reference List

- Abegg MH, Savic N, Ehrenguber MU, McKinney RA, Gahwiler BH. Epileptiform activity in rat hippocampus strengthens excitatory synapses. *J Physiol.* 2004; 554:439–448. [PubMed: 14594985]
- Arnold FJ, Hofmann F, Bengtson CP, Wittmann M, Vanhoutte P, Bading H. Microelectrode array recordings of cultured hippocampal networks reveal a simple model for transcription and protein synthesis-dependent plasticity. *J Physiol.* 2005; 564:3–19. [PubMed: 15618268]
- Bains JS, Longacher JM, Staley KJ. Reciprocal interactions between CA3 network activity and strength of recurrent collateral synapses. *Nat Neurosci.* 1999; 2:720–726. [PubMed: 10412061]
- Bartha AI, Shen J, Katz KH, Mischel RE, Yap KR, Ivacko JA, Andrews EM, Ferriero DM, Ment LR, Silverstein FS. Neonatal seizures: multicenter variability in current treatment practices. *Pediatr Neurol.* 2007; 37:85–90. [PubMed: 17675022]
- Ben-Ari Y, Gaiarsa JL, Tyzio R, Khazipov R. GABA: a pioneer transmitter that excites immature neurons and generates primitive oscillations. *Physiol Rev.* 2007; 87:1215–1284. [PubMed: 17928584]
- Ben-Ari Y, Gho M. Long-lasting modification of the synaptic properties of rat CA3 hippocampal neurones induced by kainic acid. *J Physiol.* 1988; 404:365–384. [PubMed: 2908124]
- Berglund K, Schleich W, Wang H, Feng G, Hall WC, Kuner T, Augustine GJ. Imaging synaptic inhibition throughout the brain via genetically targeted Clomeleon. *Brain Cell Biol.* 2008; 36:101–118. [PubMed: 18850274]
- Blaesse P, Airaksinen MS, Rivera C, Kaila K. Cation-chloride cotransporters and neuronal function. *Neuron.* 2009; 61:820–838. [PubMed: 19323993]
- Brumback AC, Staley KJ. Thermodynamic regulation of NKCC1-mediated Cl⁻ cotransport underlies plasticity of GABA(A) signaling in neonatal neurons. *J Neurosci.* 2008; 28:1301–1312. [PubMed: 18256250]
- Cancedda L, Fiumelli H, Chen K, Poo MM. Excitatory GABA action is essential for morphological maturation of cortical neurons in vivo. *J Neurosci.* 2007; 27:5224–5235. [PubMed: 17494709]
- Carmo KB, Barr P. Drug treatment of neonatal seizures by neonatologists and paediatric neurologists. *J Paediatr Child Health.* 2005; 41:313–316. [PubMed: 16014133]
- Cohen I, Miles R. Contributions of intrinsic and synaptic activities to the generation of neuronal discharges in in vitro hippocampus. *J Physiol.* 2000; 2(524 Pt):485–502. [PubMed: 10766928]
- Cohen I, Navarro V, Clemenceau S, Baulac M, Miles R. On the origin of interictal activity in human temporal lobe epilepsy in vitro. *Science.* 2002; 298:1418–1421. [PubMed: 12434059]
- Connell J, Oozeer R, de Vries L, Dubowitz LM, Dubowitz V. Clinical and EEG response to anticonvulsants in neonatal seizures. *Arch Dis Child.* 1989; 64:459–464. [PubMed: 2730114]
- Cowan F, Rutherford M, Groenendaal F, Eken P, Mercuri E, Bydder GM, Meiners LC, Dubowitz LM, de Vries LS. Origin and timing of brain lesions in term infants with neonatal encephalopathy. *Lancet.* 2003; 361:736–742. [PubMed: 12620738]
- Dai Y, Tang J, Zhang JH. Role of Cl⁻ in cerebral vascular tone and expression of Na⁺-K⁺-2Cl⁻ cotransporter after neonatal hypoxia-ischemia. *Can J Physiol Pharmacol.* 2005; 83:767–773. [PubMed: 16333378]
- Darman RB, Forbush B. A regulatory locus of phosphorylation in the N terminus of the Na-K-Cl cotransporter, NKCC1. *J Biol Chem.* 2002; 277:37542–37550. [PubMed: 12145304]

- Delpire E. Cation-Chloride Cotransporters in Neuronal Communication. *News Physiol Sci.* 2000; 15:309–312. [PubMed: 11390932]
- Derchansky M, Jahromi SS, Mamani M, Shin DS, Sik A, Carlen PL. Transition to seizures in the isolated immature mouse hippocampus: a switch from dominant phasic inhibition to dominant phasic excitation. *J Physiol.* 2008; 586:477–494. [PubMed: 17991696]
- Duebel J, Haverkamp S, Schleich W, Feng G, Augustine GJ, Kuner T, Euler T. Two-photon imaging reveals somatodendritic chloride gradient in retinal ON-type bipolar cells expressing the biosensor Clomeleon. *Neuron.* 2006; 49:81–94. [PubMed: 16387641]
- Dzhala VI, Brumback AC, Staley KJ. Bumetanide enhances phenobarbital efficacy in a neonatal seizure model. *Ann Neurol.* 2008; 63:222–235. [PubMed: 17918265]
- Dzhala VI, Staley KJ. Excitatory Actions of Endogenously Released GABA Contribute to Initiation of Ictal Epileptiform Activity in the Developing Hippocampus. *J Neurosci.* 2003; 23:1840–1846. [PubMed: 12629188]
- Dzhala VI, Talos DM, Sdrulla DA, Brumback AC, Mathews GC, Benke TA, Delpire E, Jensen FE, Staley KJ. NKCC1 transporter facilitates seizures in the developing brain. *Nat Med.* 2005; 11:1205–1213. [PubMed: 16227993]
- Fisher RS, Pedley TA, Moody WJ Jr, Prince DA. The role of extracellular potassium in hippocampal epilepsy. *Arch Neurol.* 1976; 33:76–83. [PubMed: 1252153]
- Fiumelli H, Woodin MA. Role of activity-dependent regulation of neuronal chloride homeostasis in development. *Curr Opin Neurobiol.* 2007; 17:81–86. [PubMed: 17234400]
- Flemmer AW, Gimenez I, Dowd BF, Darman RB, Forbush B. Activation of the Na-K-Cl cotransporter NKCC1 detected with a phospho-specific antibody. *J Biol Chem.* 2002; 277:37551–37558. [PubMed: 12145305]
- Gagnon KB, England R, Diehl L, Delpire E. Apoptosis-associated tyrosine kinase scaffolding of protein phosphatase 1 and SPAK reveals a novel pathway for Na-K-2Cl cotransporter regulation. *Am J Physiol Cell Physiol.* 2007; 292:C1809–C1815. [PubMed: 17267545]
- Galanopoulou AS. Dissociated gender-specific effects of recurrent seizures on GABA signaling in CA1 pyramidal neurons: role of GABA(A) receptors. *J Neurosci.* 2008; 28:1557–1567. [PubMed: 18272677]
- Gamba G. Molecular physiology and pathophysiology of electroneutral cation-chloride cotransporters. *Physiol Rev.* 2005; 85:423–493. [PubMed: 15788703]
- Ge S, Goh ELK, Sailor KA, Kitabatake Y, Ming GI, Song H. GABA regulates synaptic integration of newly generated neurons in the adult brain. *Nature.* 2006; 439:589–593. [PubMed: 16341203]
- Gimenez I, Forbush B. Short-term stimulation of the renal Na-K-Cl cotransporter (NKCC2) by vasopressin involves phosphorylation and membrane translocation of the protein. *J Biol Chem.* 2003; 278:26946–26951. [PubMed: 12732642]
- Glykys J, Dzhala VI, Kuchibhotla KV, Feng G, Kuner T, Augustine G, Bacskai BJ, Staley KJ. Differences in cortical versus subcortical GABAergic signaling: a candidate mechanism of electroclinical uncoupling of neonatal seizures. *Neuron.* 2009; 63:657–672. [PubMed: 19755108]
- Goodkin HP, Joshi S, Mchedlishvili Z, Brar J, Kapur J. Subunit-specific trafficking of GABA(A) receptors during status epilepticus. *J Neurosci.* 2008; 28:2527–2538. [PubMed: 18322097]
- Hannaert P, Alvarez-Guerra M, Pirot D, Nazaret C, Garay RP. Rat NKCC2/NKCC1 cotransporter selectivity for loop diuretic drugs. *Naunyn Schmiedeberg Arch Pharmacol.* 2002; 365:193–199. [PubMed: 11882915]
- Haugvicova R, Kubova H, Mares P. Antipentylentetrazol action of clobazam in developing rats. *Physiol Res.* 1999; 48:501–507. [PubMed: 10783916]
- Heinemann U, Lux HD, Gutnick MJ. Extracellular free calcium and potassium during paroxysmal activity in the cerebral cortex of the cat. *Exp Brain Res.* 1977; 27:237–243. [PubMed: 880984]
- Hirsch JC, Agassandian C, Merchan-Perez A, Ben-Ari Y, DeFelipe J, Esclapez M, Bernard C. Deficit of quantal release of GABA in experimental models of temporal lobe epilepsy. *Nat Neurosci.* 1999; 2:499–500. [PubMed: 10448211]
- Ikonomidou C. Triggers of apoptosis in the immature brain. *Brain Dev.* 2009; 31:488–492. [PubMed: 19307071]

- Isaev D, Isaeva E, Khazipov R, Holmes GL. Shunting and hyperpolarizing GABAergic inhibition in the high-potassium model of ictogenesis in the developing rat hippocampus. *Hippocampus*. 2007; 17:210–219. [PubMed: 17294460]
- Isenring P, Jacoby SC, Payne JA, Forbush B III. Comparison of Na-K-Cl cotransporters. NKCC1, NKCC2, and the HEK cell Na-L-Cl cotransporter. *J Biol Chem*. 1998; 273:11295–11301. [PubMed: 9556622]
- Jin X, Huguenard JR, Prince DA. Impaired Cl⁻ extrusion in layer V pyramidal neurons of chronically injured epileptogenic neocortex. *J Neurophysiol*. 2005; 93:2117–2126. [PubMed: 15774713]
- Kahle KT, Staley KJ, Nahed BV, Gamba G, Hebert SC, Lifton RP, Mount DB. Roles of the cation-chloride cotransporters in neurological disease. *Nat Clin Pract Neurol*. 2008; 4:490–503. [PubMed: 18769373]
- Khalilov I, Dzhala V, Ben Ari Y, Khazipov R. Dual role of GABA in the neonatal rat hippocampus. *Dev Neurosci*. 1999a; 21:310–319. [PubMed: 10575254]
- Khalilov I, Dzhala V, Medina I, Leinekugel X, Melyan Z, Lamsa K, Khazipov R, Ben Ari Y. Maturation of kainate-induced epileptiform activities in interconnected intact neonatal limbic structures in vitro. *Eur J Neurosci*. 1999b; 11:3468–3480. [PubMed: 10564355]
- Khalilov I, Esclapez M, Medina I, Aggoun D, Lamsa K, Leinekugel X, Khazipov R, Ben Ari Y. A novel in vitro preparation: the intact hippocampal formation. *Neuron*. 1997; 19:743–749. [PubMed: 9354321]
- Khalilov I, Holmes GL, Ben-Ari Y. In vitro formation of a secondary epileptogenic mirror focus by interhippocampal propagation of seizures. *Nat Neurosci*. 2003; 6:1079–1085. [PubMed: 14502289]
- Khazipov R, Khalilov I, Tyzio R, Morozova E, Ben Ari Y, Holmes GL. Developmental changes in GABAergic actions and seizure susceptibility in the rat hippocampus. *Eur J Neurosci*. 2004; 19:590–600. [PubMed: 14984409]
- Kilb W, Sinning A, Luhmann HJ. Model-specific effects of bumetanide on epileptiform activity in the in-vitro intact hippocampus of the newborn mouse. *Neuropharmacology*. 2007; 53:524–533. [PubMed: 17681355]
- Kuner T, Augustine GJ. A genetically encoded ratiometric indicator for chloride: capturing chloride transients in cultured hippocampal neurons. *Neuron*. 2000; 27:447–459. [PubMed: 11055428]
- Li X, Zhou J, Chen Z, Chen S, Zhu F, Zhou L. Long-term expressional changes of Na(+)-K(+)-Cl(-) co-transporter 1 (NKCC1) and K(+)-Cl(-) co-transporter 2 (KCC2) in CA1 region of hippocampus following lithium-pilocarpine induced status epilepticus (PISE). *Brain Res*. 2008; 1221:141–146. [PubMed: 18550034]
- Mazarati A, Shin D, Sankar R. Bumetanide inhibits rapid kindling in neonatal rats. *Epilepsia*. 2009
- Mizrahi EM, Kellaway P. Characterization and classification of neonatal seizures. *Neurology*. 1987; 37:1837–1844. [PubMed: 3683874]
- Moody WJ, Futamachi KJ, Prince DA. Extracellular potassium activity during epileptogenesis. *Exp Neurol*. 1974; 42:248–263. [PubMed: 4824976]
- Nabekura J, Ueno T, Okabe A, Furuta A, Iwaki T, Shimizu-Okabe C, Fukuda A, Akaike N. Reduction of KCC2 expression and GABAA receptor-mediated excitation after in vivo axonal injury. *J Neurosci*. 2002; 22:4412–4417. [PubMed: 12040048]
- Nardou R, Ben-Ari Y, Khalilov I. Bumetanide, an NKCC1 Antagonist, Does Not Prevent Formation of Epileptogenic Focus but Blocks Epileptic Focus Seizures in Immature Rat Hippocampus. *J Neurophysiol*. 2009
- Naylor DE, Liu H, Wasterlain CG. Trafficking of GABA(A) receptors, loss of inhibition, and a mechanism for pharmacoresistance in status epilepticus. *J Neurosci*. 2005; 25:7724–7733. [PubMed: 16120773]
- Painter MJ, Scher MS, Stein AD, Armatti S, Wang Z, Gardiner JC, Paneth N, Minnigh B, Alvin J. Phenobarbital compared with phenytoin for the treatment of neonatal seizures. *N Engl J Med*. 1999; 341:485–489. [PubMed: 10441604]
- Pathak HR, Weissinger F, Terunuma M, Carlson GC, Hsu FC, Moss SJ, Coulter DA. Disrupted dentate granule cell chloride regulation enhances synaptic excitability during development of temporal lobe epilepsy. *J Neurosci*. 2007; 27:14012–14022. [PubMed: 18094240]

- Payne JA. Functional characterization of the neuronal-specific K-Cl cotransporter: implications for [K⁺]_o regulation. *Am J Physiol.* 1997; 273:C1516–C1525. [PubMed: 9374636]
- Payne JA, Rivera C, Voipio J, Kaila K. Cation-chloride co-transporters in neuronal communication, development and trauma. *Trends Neurosci.* 2003; 26:199–206. [PubMed: 12689771]
- Pond BB, Berglund K, Kuner T, Feng G, Augustine GJ, Schwartz-Bloom RD. The chloride transporter Na⁺-K⁺-Cl⁻ cotransporter isoform-1 contributes to intracellular chloride increases after in vitro ischemia. *J Neurosci.* 2006; 26:1396–1406. [PubMed: 16452663]
- Prince DA, Lux HD, Neher E. Measurement of extracellular potassium activity in cat cortex. *Brain Res.* 1973; 50:489–495. [PubMed: 4705519]
- Qian N, Sejnowski TJ. When is an inhibitory synapse effective? *Proc Natl Acad Sci U S A.* 1990; 87:8145–8149. [PubMed: 2236028]
- Quilichini PP, Diabira D, Chiron C, Ben-Ari Y, Gozlan H. Persistent epileptiform activity induced by low Mg²⁺ in intact immature brain structures. *Eur J Neurosci.* 2002; 16:850–860. [PubMed: 12372021]
- Quilichini PP, Diabira D, Chiron C, Milh M, Ben-Ari Y, Gozlan H. Effects of antiepileptic drugs on refractory seizures in the intact immature corticohippocampal formation in vitro. *Epilepsia.* 2003; 44:1365–1374. [PubMed: 14636342]
- Raol YH, Lapidés DA, Keating JG, Brooks-Kayal AR, Cooper EC. A KCNQ channel opener for experimental neonatal seizures and status epilepticus. *Ann Neurol.* 2009; 65:326–336. [PubMed: 19334075]
- Rennie JM, Boylan GB. Neonatal seizures and their treatment. *Curr Opin Neurol.* 2003; 16:177–181. [PubMed: 12644746]
- Rheims S, Minlebaev M, Ivanov A, Represa A, Khazipov R, Holmes GL, Ben-Ari Y, Zilberter Y. Excitatory GABA in Rodent Developing Neocortex in vitro. *J Neurophysiol.* 2008
- Schneiderman JH, Sterling CA, Luo R. Hippocampal plasticity following epileptiform bursting produced by GABAA antagonists. *Neuroscience.* 1994; 59:259–273. [PubMed: 7911981]
- Sipila ST, Schuchmann S, Voipio J, Yamada J, Kaila K. The cation-chloride cotransporter NKCC1 promotes sharp waves in the neonatal rat hippocampus. *J Physiol.* 2006; 573:765–773. [PubMed: 16644806]
- Staley K, Smith R. A new form of feedback at the GABA(A) receptor. *Nat Neurosci.* 2001; 4:674–676. [PubMed: 11426214]
- Staley KJ, Mody I. Shunting of excitatory input to dentate gyrus granule cells by a depolarizing GABAA receptor-mediated postsynaptic conductance. *J Neurophysiol.* 1992; 68:197–212. [PubMed: 1381418]
- Staley KJ, Proctor WR. Modulation of mammalian dendritic GABA(A) receptor function by the kinetics of Cl⁻ and. *J Physiol.* 1999; 3(519 Pt):693–712. [PubMed: 10457084]
- Stein V, Hermans-Borgmeyer I, Jentsch TJ, Hubner CA. Expression of the KCl cotransporter KCC2 parallels neuronal maturation and the emergence of low intracellular chloride. *J Comp Neurol.* 2004; 468:57–64. [PubMed: 14648690]
- Stosiek C, Garaschuk O, Holthoff K, Konnerth A. In vivo two-photon calcium imaging of neuronal networks. *Proc Natl Acad Sci U S A.* 2003; 100:7319–7324. [PubMed: 12777621]
- Sun D, Murali SG. Stimulation of Na⁺-K⁺-2Cl⁻ cotransporter in neuronal cells by excitatory neurotransmitter glutamate. *Am J Physiol.* 1998; 275:C772–C779. [PubMed: 9730961]
- Tekgul H, Gauvreau K, Soul J, Murphy L, Robertson R, Stewart J, Volpe J, Bourgeois B, du Plessis AJ. The current etiologic profile and neurodevelopmental outcome of seizures in term newborn infants. *Pediatrics.* 2006; 117:1270–1280. [PubMed: 16585324]
- Thompson SM, Gahwiler BH. Activity-dependent disinhibition. II. Effects of extracellular potassium, furosemide, and membrane potential on Cl⁻ in hippocampal CA3 neurons. *J Neurophysiol.* 1989; 61:512–523. [PubMed: 2709097]
- Twyman RE, Rogers CJ, Macdonald RL. Differential regulation of gamma-aminobutyric acid receptor channels by diazepam and phenobarbital. *Ann Neurol.* 1989; 25:213–220. [PubMed: 2471436]
- Tyzio R, Holmes GL, Ben-Ari Y, Khazipov R. Timing of the developmental switch in GABA(A) mediated signaling from excitation to inhibition in CA3 rat hippocampus using gramicidin

- perforated patch and extracellular recordings. *Epilepsia*. 2007; 5(48 Suppl):96–105. [PubMed: 17910587]
- Tyzio R, Ivanov A, Bernard C, Holmes GL, Ben Ari Y, Khazipov R. Membrane potential of CA3 hippocampal pyramidal cells during postnatal development. *J Neurophysiol*. 2003; 90:2964–2972. [PubMed: 12867526]
- Tyzio R, Cossart R, Khalilov I, Minlebaev M, Hubner CA, Represa A, Ben-Ari Y, Khazipov R. Maternal oxytocin triggers a transient inhibitory switch in GABA signaling in the fetal brain during delivery. *Science*. 2006; 314:1788–1792. [PubMed: 17170309]
- van den Pol AN, Obrietan K, Chen G. Excitatory actions of GABA after neuronal trauma. *J Neurosci*. 1996; 16:4283–4292. [PubMed: 8753889]
- Velisek L, Veliskova J, Ptachewich Y, Ortiz J, Shinnar S, Moshe SL. Age-dependent effects of gamma-aminobutyric acid agents on flurothyl seizures. *Epilepsia*. 1995; 36:636–643. [PubMed: 7555978]
- Volpe, JJ. *Neurology of the newborn*. Saunders; Philadelphia: 2001.
- Wang C, Shimizu-Okabe C, Watanabe K, Okabe A, Matsuzaki H, Ogawa T, Mori N, Fukuda A, Sato K. Developmental changes in KCC1, KCC2, and NKCC1 mRNA expressions in the rat brain. *Brain Res Dev Brain Res*. 2002; 139:59–66.
- Wang DD, Kriegstein AR, Ben-Ari Y. GABA Regulates Stem Cell Proliferation before Nervous System Formation. *Epilepsy Curr*. 2008; 8:137–139. [PubMed: 18852839]
- Wells JE, Porter JT, Agmon A. GABAergic inhibition suppresses paroxysmal network activity in the neonatal rodent hippocampus and neocortex. *J Neurosci*. 2000; 20:8822–8830. [PubMed: 11102490]
- Woodin MA, Ganguly K, Poo MM. Coincident pre- and postsynaptic activity modifies GABAergic synapses by postsynaptic changes in Cl⁻ transporter activity. *Neuron*. 2003; 39:807–820. [PubMed: 12948447]
- Xiong ZQ, Saggau P, Stringer JL. Activity-dependent intracellular acidification correlates with the duration of seizure activity. *J Neurosci*. 2000; 20:1290–1296. [PubMed: 10662818]
- Xiong ZQ, Stringer JL. Sodium pump activity, not glial spatial buffering, clears potassium after epileptiform activity induced in the dentate gyrus. *J Neurophysiol*. 2000; 83:1443–1451. [PubMed: 10712471]
- Yamada J, Okabe A, Toyoda H, Kilb W, Luhmann HJ, Fukuda A. Cl⁻ uptake promoting depolarizing GABA actions in immature rat neocortical neurones is mediated by NKCC1. *J Physiol*. 2004; 557:829–841. [PubMed: 15090604]

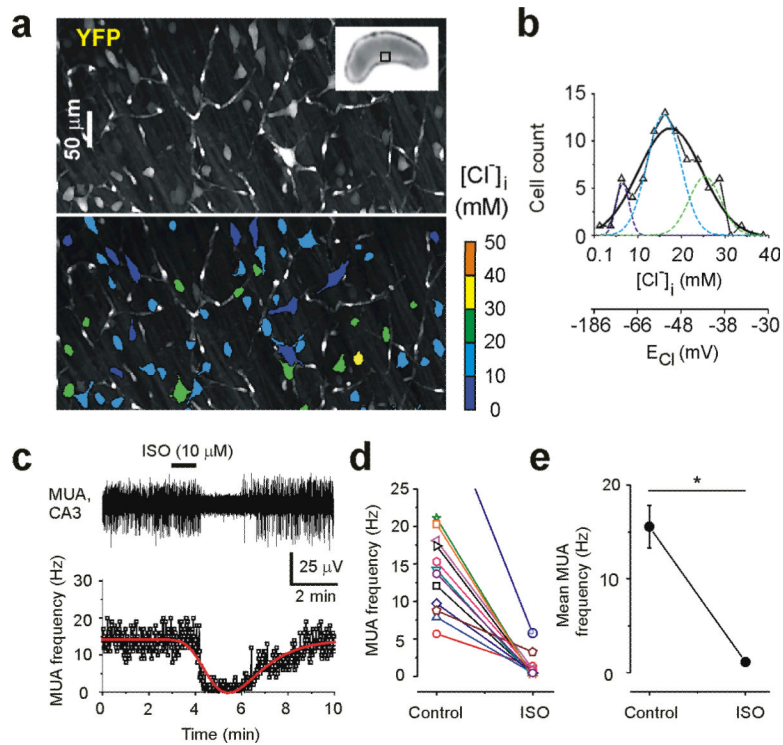


Figure 1.

Distribution of resting $[Cl^-]_i$ and GABA action in the intact neonatal hippocampus. **(a)** Two-photon fluorescence confocal scanning images of the CA3 pyramidal cell layer in the intact hippocampus *in vitro* of the neonatal (P7) transgenic CLM-1 mouse expressing Clomeleon. *Top panel*: overlay of confocal multiple planes (150 samples; 2 μ m step) of the Cl^- sensitive YFP signals of the CA3 neurons. Inset shows the photograph of the intact hippocampus. *Bottom panel*: pseudo-colored regions of interest (ROI) from neurons according to $[Cl^-]_i$. **(b)** Distribution of resting $[Cl^-]_i$ (bin size 2.5 mM) from 81 individual neurons shown in **(a)**. A Gaussian fit yielded a peak at 17.4 ± 0.6 mM and width of 14.6 ± 2.3 mM. Multi-peak fit yielded three peaks at 6.5 ± 0.6 mM, 15.9 ± 1 mM and 25.3 ± 2.1 mM. **(c–e)** Effect of isoguvacine (ISO) on multiple-unit activity (MUA) in the intact neonatal (P5–7) hippocampal preparations. **(c)** Extracellular recording of MUA in the CA3 pyramidal cell layer and corresponding frequency of MUA. Bath application of isoguvacine (10 μ M) caused a transient decrease in the frequency of MUA; peak function fit is indicated by red line. **(d–e)** Individual hippocampus responses to isoguvacine and corresponding mean frequency of MUA (* $p=0.00002$, two sample t-Test). Decrease in MUA frequency indicates that the net effect of $GABA_A$ -R activation was inhibitory.

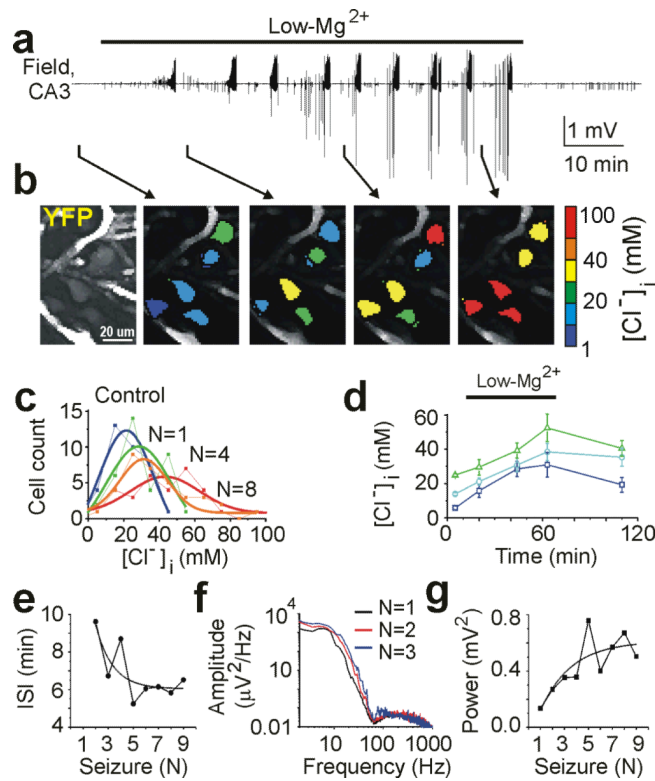


Figure 2.

Neonatal seizure-induced chloride accumulation and facilitation of recurrent seizures. **(a)** Extracellular field potential recordings in the CA3 pyramidal cell layer in the intact hippocampus *in vitro* of the neonatal (P5) CLM-1 mouse. Recurrent seizures were induced by low-Mg²⁺ ACSF and stopped by perfusion of control ACSF. **(b)** Effect of recurrent seizures on [Cl⁻]_i. Example of two-photon confocal imaging of YFP (*left*) of CA3 neurons yielded pseudo-color map of [Cl⁻]_i before seizures, after the first, fourth and eighth recurrent seizures. **(c)** Distribution of [Cl⁻]_i (bin size 10 mM) in 36 identified neurons before seizures (*dark blue*), after one (*green*), four (*orange*) and eight (*red*) recurrent seizures. **(d)** Corresponding changes of mean [Cl⁻]_i in subpopulation of neurons with low (0–10 mM), medium (10–20 mM) and high (20–30 mM) range of control resting chloride. **(e – g)** Seizure induced facilitation of recurrent seizures. **(e)** Inter-seizure intervals decreased as a function of the number of recurrent seizures. **(f)** Power spectra of three consecutive seizures in frequency band from 1 to 1000 Hz. **(g)** Corresponding power of recurrent seizures as a function of the number of seizures.

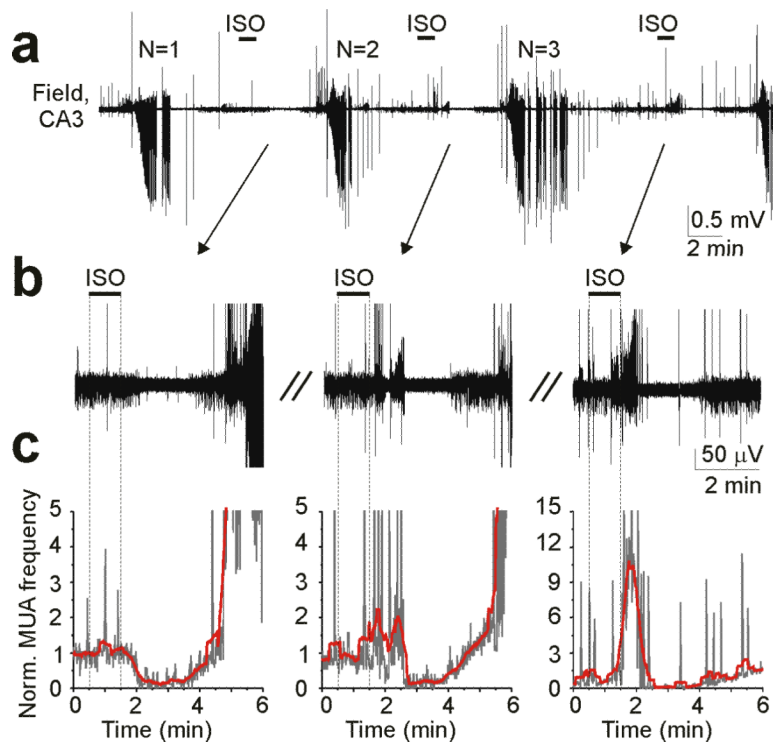
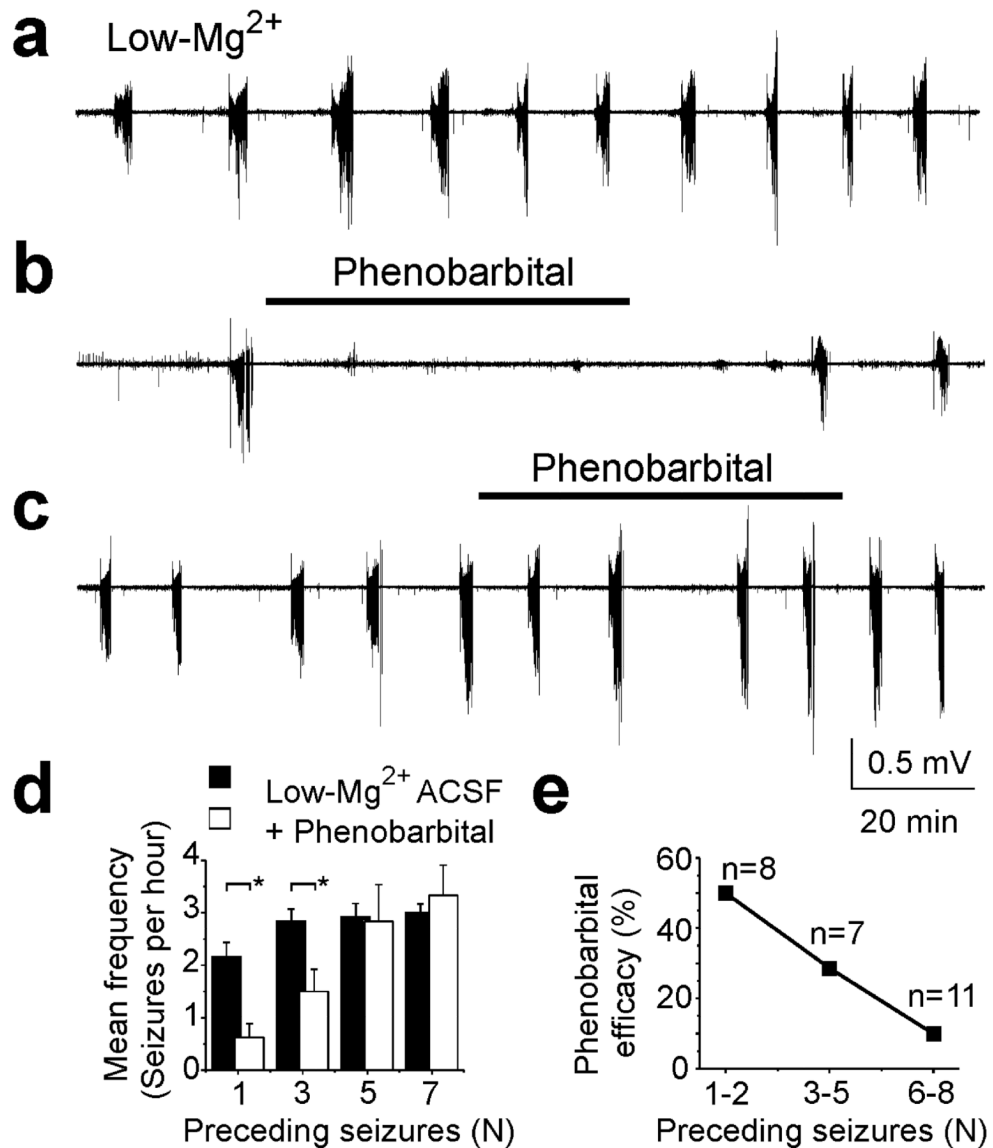


Figure 3.

Seizure-dependent changes in the effects of the GABA_A agonist isoguvacine on MUA and epileptiform discharges. (a–b) Extracellular field potential recordings in the CA3 pyramidal cell layer in the intact hippocampus *in vitro* of the neonatal (P5) CLM-1 mouse. Recurrent seizures were induced by low-Mg²⁺ ACSF. Application of isoguvacine (ISO; 10 μM for 1 min) after N=1 seizure decreased neuronal firing. Similar applications of isoguvacine after N=2 and N=3 seizures transiently increased neuronal firing rate in association with a transient increase of the frequency of interictal epileptiform discharges (IEDs). (c) Corresponding normalized frequency of MUA. Excitatory action of isoguvacine increased as a function of recurrent seizures. Red lines represent adjacent averaging of 20 data points. Vertical dashed lines on (b) and (c) panels delineate isoguvacine application.

**Figure 4.**

Seizure-dependent changes in the effects of phenobarbital on neonatal seizures. (a) Low-Mg²⁺ ACSF – induced recurrent seizures in the intact hippocampus *in vitro*. (b) Application of phenobarbital (100 μM) in low-Mg²⁺ ACSF after one ictal-like event (N=1) abolished seizures in the intact neonatal hippocampus. (c) Application of phenobarbital (100 μM) after five ictal-like events (N=5) failed to abolish recurrent ictal-like activity in low-Mg²⁺ ACSF. (a–c) Extracellular field potential recordings were performed in the CA3 pyramidal cell layer in the intact hippocampus *in vitro* of neonatal (P5–6) rats. (d) Frequency of recurrent seizures as a function of preceding seizures (N) in control low-Mg²⁺ ACSF and after application of phenobarbital. Phenobarbital applied after N=1 and N=3 seizures significantly reduced the mean frequency of recurrent seizures (*p < 0.05). Phenobarbital applied after more than N=5 seizures failed to reduce the frequency of recurrent seizures. (e) Fraction of hippocampi in low-Mg²⁺ ACSF in which seizures were abolished by 100 μM phenobarbital, plotted as a function of the number of seizures prior to Phenobarbital application. Efficacy of phenobarbital in neonatal seizures decreased as a function of quantity of prior seizure activity (N).

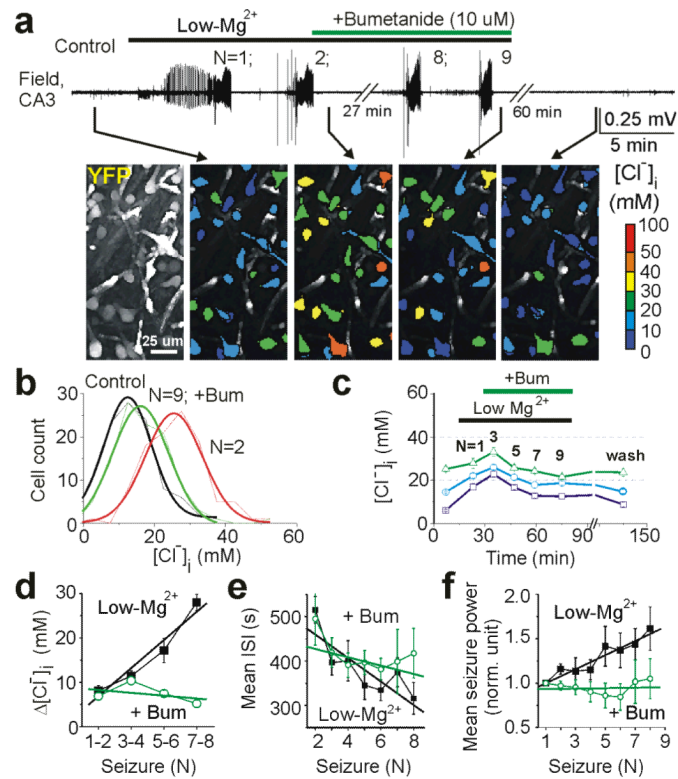


Figure 5.

The role of NKCC1 in seizure-induced chloride accumulation and facilitation of recurrent seizures. **(a)** Top: low- Mg^{2+} ACSF induced recurrent seizures in control and in the presence of NKCC1 blocker bumetanide ($10 \mu M$). Extracellular field potential recordings in the CA3 pyramidal cell layer in the intact hippocampus *in vitro* of neonatal (P5) CLM-1 mouse. Bottom: example of two-photon confocal imaging of YFP (*left*) of CA3 neurons yielded pseudo-color map of $[Cl^-]_i$ before seizures, after two seizures, and after nine seizures in presence of bumetanide. **(b)** Distribution of $[Cl^-]_i$ (bin size 10 mM) in 48 identified neurons before seizures (*black*), after two seizures in control (low Mg) solution (*red*), and after nine seizures in the presence of bumetanide (*green*). Gauss fits yielded mean \pm width values of 22.1 ± 19 mM in control, 29.8 ± 18.4 mM after N=2 seizures, and 44.4 ± 24.1 mM after N=9 seizures. **(c)** Seizure-induced changes of mean $[Cl^-]_i$ in subpopulation of neurons with low (0–10 mM), medium (10–20 mM) and high (20–30 mM) range of control resting chloride. Bumetanide prevented seizure-induced neuronal chloride accumulation. **(d)** Effects of recurrent seizures on intracellular chloride accumulation in control low- Mg^{2+} ACSF and in the presence of bumetanide. Solid lines represent linear regression (Control, low- Mg^{2+} ACSF [black]: $r = 0.97 \pm 1.66$; $p = 0.03$; Bumetanide [green]: $r = -0.43 \pm 2.6$; $p = 0.57$). In low- Mg^{2+} ACSF, $[Cl^-]_i$ progressively increases as a function of recurrent seizures. Bumetanide prevents progressive chloride accumulation induced by recurrent seizures. **(e–f)** Mean inter-seizure intervals **(e)** and seizure power **(f)** as a function of the number of recurrent seizures. **(e)** Solid lines represent linear regression fit of the mean inter-seizure intervals (ISIs) in control (black; $r = -0.82 \pm 1.37$; $p = 0.02$) and in the presence of bumetanide (green: $r = -0.55 \pm 0.7$; $p = 0.2$). **(f)** Corresponding linear regression fit of normalized mean power in control (black: $r = 0.95 \pm 0.07$; $p = 0.0003$; $n = 8$) and in the presence of bumetanide (green: $r = 0.08 \pm 0.08$; $p = 0.85$; $n = 8$). Bumetanide prevents a progressive increase of seizure power and frequency.

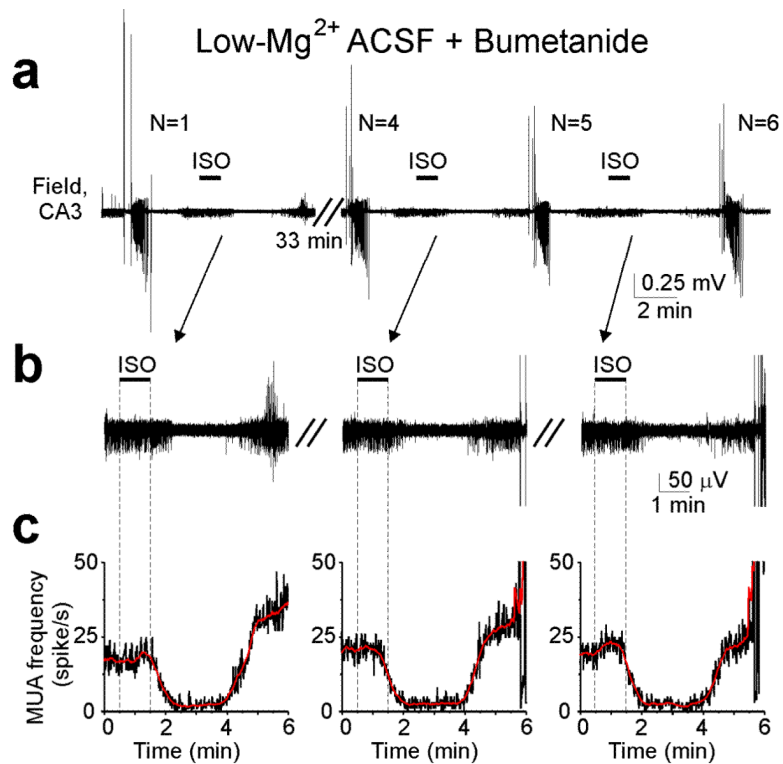
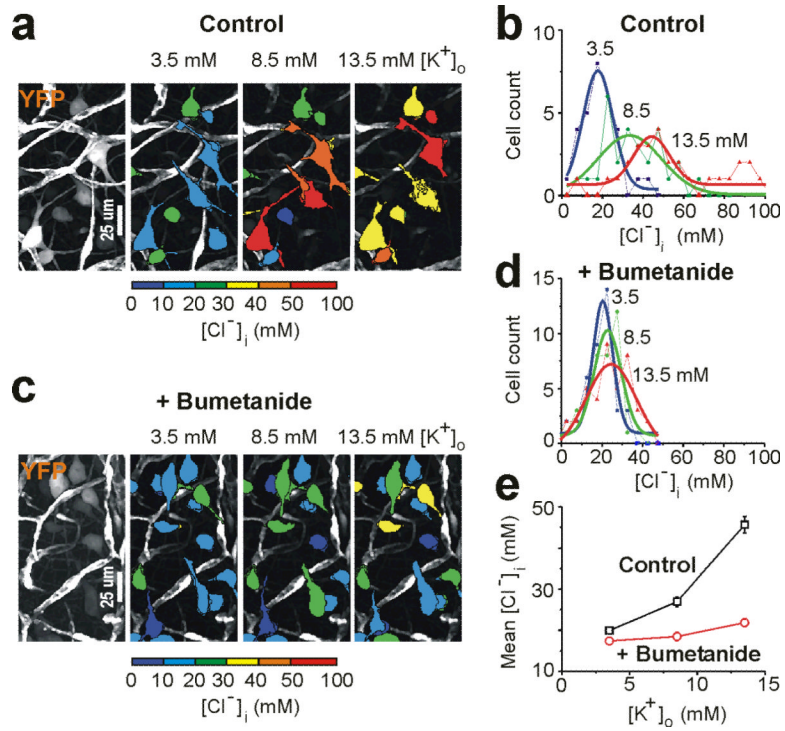


Figure 6.

The role of NKCC1 in seizure-induced changes in the action of GABA. (a–b) Extracellular field potential recordings in the CA3 pyramidal cell layer in the intact hippocampus *in vitro* of the neonatal (P5) mouse. Recurrent seizures were induced by low-Mg²⁺ ACSF in the presence of NKCC1 blocker bumetanide (10 μM). Applications of isoguvacine (ISO; 10 μM for 1 min) after seizure and recovery from post-ictal depression transiently decreased neuronal firing rate. (c) Corresponding frequency of MUA. Vertical dashed lines delineate isoguvacine application. Red lines represent adjacent averaging of 20 data points. Bumetanide prevented seizure-induced changes in the effects of the GABA_A-R agonist isoguvacine on MUA and epileptiform discharges (Fig. 3).

**Figure 7.**

Concentration gradient of potassium regulates NKCC1 activity. **(a–e)** Changes in intracellular chloride distribution as a function of extracellular concentration of potassium ($[K^+]_o$) in the presence of sodium channel blocker TTX (1μ M). **(a, c)** Examples of two-photon confocal imaging of YFP (*left*) of CA3 neurons yielded pseudo-color map of $[Cl^-]_i$ at different $[K^+]_o$ (3.5 mM, 8.5 mM and 13.5 mM) in control **(a)** and in presence of bumetanide **(c)**. **(b, d)** Corresponding distributions of $[Cl^-]_i$ (bin size 5 mM) in control **(b; n = 30** identified neurons) and in the presence of bumetanide **(d; n = 40** identified neurons). Data were fitted with a Gaussian function. **(e)** Mean $[Cl^-]_i$ as a function of $[K^+]_o$ in control and in the presence of bumetanide.

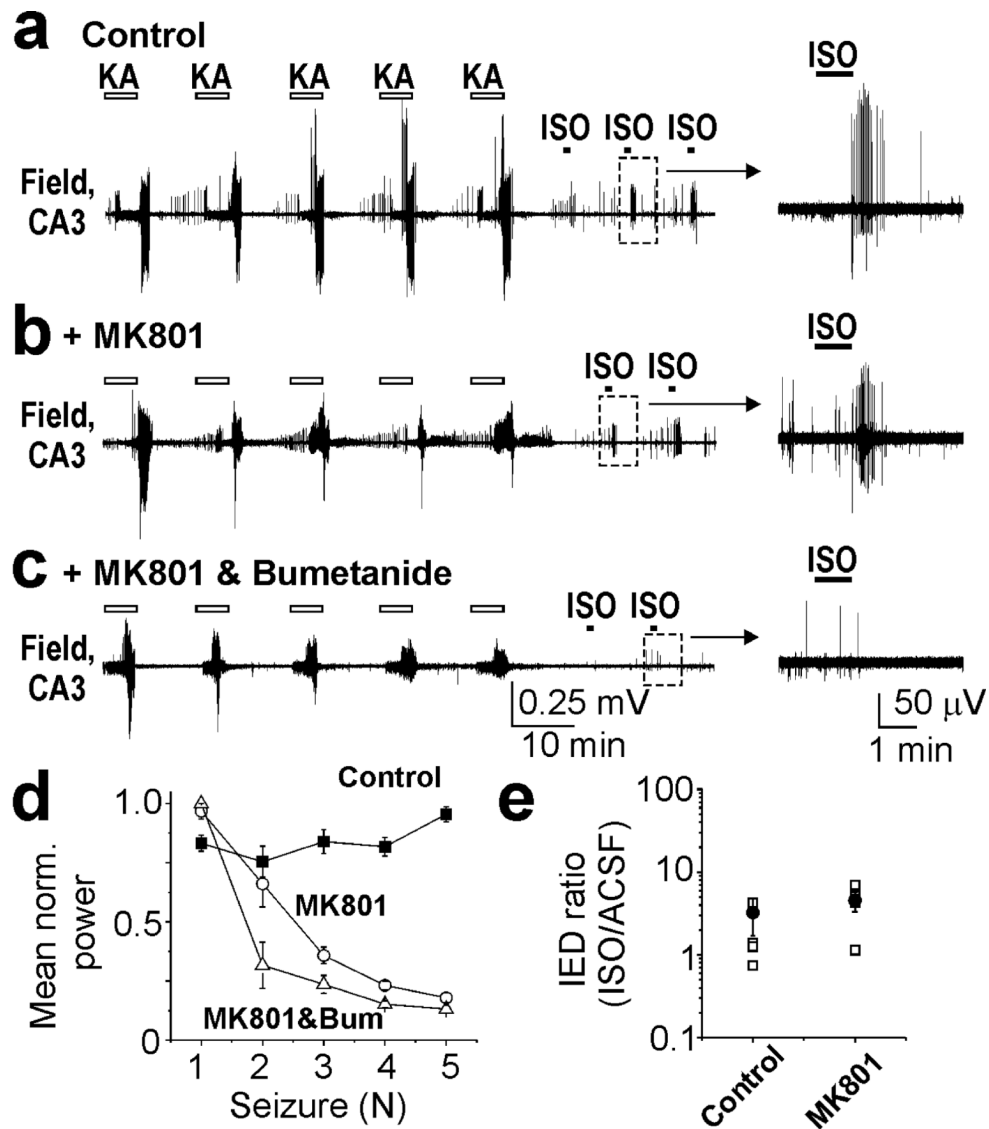


Figure 8. Seizure-induced changes in the action of GABA are NMDA receptor independent. **(a)** Repetitive applications of kainic acid (KA; 1 μ M for 5 min; *opened bars*) induced ictal-like epileptiform discharges (seizures) followed by spontaneous interictal epileptiform discharges (IEDs). Brief applications of isoguvacine (ISO; 10 μ M for 1 min; *solid bars*) transiently increased the frequency of IEDs. **(b)** Perfusion of the non-competitive NMDA receptor antagonist MK801 (20 μ M) depressed KA- induced seizures. Applications of isoguvacine increased the frequency of spontaneous IEDs. **(c)** Simultaneous perfusion of MK801 and bumetanide (10 μ M) strongly depressed KA-induced seizures and prevented excitatory shift in the action of GABA. Applications of isoguvacine reduced the frequency of MUA and/or IEDs. **(a–c)** Extracellular field potential recordings in the CA3 pyramidal cell layer in the intact hippocampus of neonatal (P5–6) mice. **(d)** Normalized power of KA-induced seizures (mean \pm se) in control (squares), in the presence of MK801 (circles), and both MK801 and bumetanide (triangles). **(e)** Effects of isoguvacine on the frequency of spontaneous IEDs.

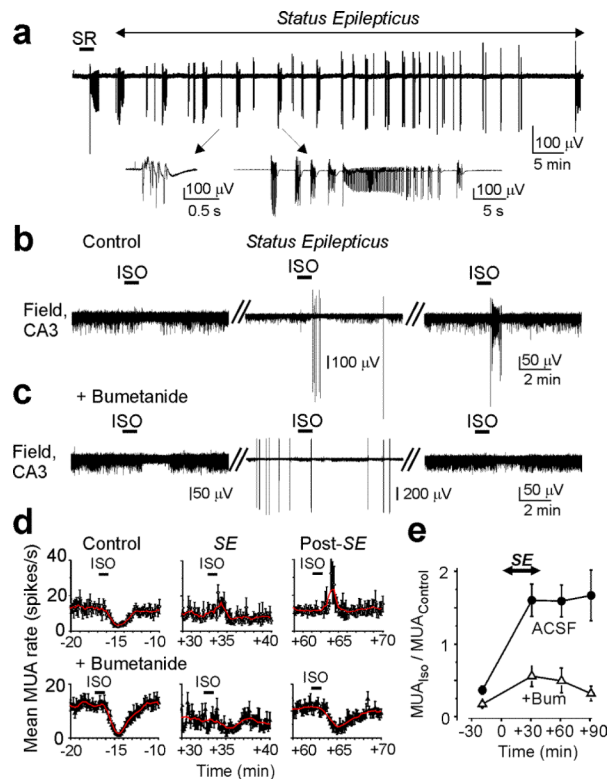


Figure 9.

Recurrent seizures invert the effects of GABA_A receptors via NKCC1-dependent mechanism. (a) Spontaneous seizures (Status epilepticus) were induced by brief bath application of the GABA_A receptor antagonist SR95531 (10 μM). In the lower panel, spontaneous epileptiform discharges are shown on an expanded time scale. (b–c) Effects of the GABA_A-R agonist isoguvacine on MUA and spontaneous epileptiform activity. In control ACSF, application isoguvacine (10 μM) decreased the frequency of MUA. 30–40 min after onset of spontaneous seizures isoguvacine increased the frequency of MUA and interictal epileptiform discharges. Excitatory effects of isoguvacine on population activity persisted at least 1–2 hours after termination of seizures. (c) Bumetanide (10 μM) prevented the excitatory action of isoguvacine on the MUA and interictal epileptiform discharges. (a–c) Extracellular recordings of MUA and population activity were performed in the CA3 pyramidal cell layer of intact neonatal (P4–5) hippocampal preparations *in vitro*. (d, e) Mean frequency of MUA in control ACSF and in the presence of bumetanide (n=6) before, during and after spontaneous seizures. (d) Time course of isoguvacine action on MUA frequency. Bumetanide (10 μM) prevented the seizure-induced reversal of the effects of GABA_A-R activation.

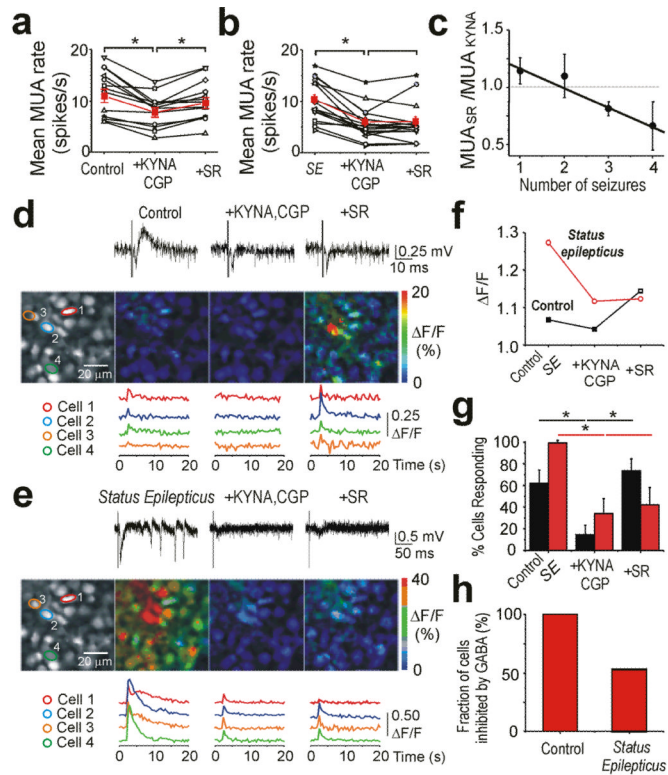


Figure 10.

Neonatal seizures alter the effect of synaptic activation of GABA_A receptors. **(a–c)** Effects on spontaneous neuronal firing rate of suppressing synaptic excitation and inhibition in control and during seizures. In control **(a)** Kynurenic acid (KYNA; 2 mM) co-applied with CGP55845 (1 μ M) reduced the mean frequency of MUA in the CA3 pyramidal cell layer in the intact neonatal hippocampi at P4–5. Subsequent application of the GABA_A-R antagonist SR95531, in the presence of KYNA and CGP, increased MUA frequency, demonstrating the net inhibitory effect of GABA_A-R when activated by endogenously released GABA. **(b)** Spontaneous seizures were induced by brief (2–3 min) application of SR95531. After 30 min of spontaneous seizure activity following washout of SR95531, application of KYNA and CGP stopped recurrent seizures and reduced MUA frequency. Subsequent application of SR95531 did not change the mean frequency of MUA. Red plots represent the averaged mean frequency of MUA. **(c)** Mean ratio of MUA frequency (SR/(KYNA+CGP)) reversed as a function of the number of seizures. Solid line represents corresponding linear regression fit ($r = -0.98$; $p = 0.02$). **(d, e)** Synchronous extracellular field potentials and two-photon fluorescence [Ca^{2+}]_i imaging in the CA3 pyramidal cell layer at P5 in the intact hippocampal preparation. Neurons were labeled by the calcium indicator dye Oregon Green BAPTA-1 AM (OGB). Field excitatory postsynaptic potentials and intracellular calcium signals were induced by electrical stimulation in the *stratum radiatum* proximal of the CA3 area. In control **(d)**, bath application of KYNA (2 mM) and GGP (1 μ M) depressed calcium signals ($\Delta F/F$) in the majority of CA3 neurons. Subsequent application of SR 95531 (10 μ M), in the presence of KYNA and CGP 55845, increased $\Delta F/F$ in the majority of the cells. The increase in Ca^{2+} in the presence of ionotropic glutamate and GABA receptor antagonists likely represents metabotropic receptor activation and direct electrical stimulation. **(e)** After spontaneous seizures, the effect of SR 95531 on $\Delta F/F$ was reversed in ~50% of neurons. **(f, g)** Mean population response ($\Delta F/F$) and fraction of cells with a stimulus-induced increase in calcium responses during applications of drugs in control and after spontaneous seizures. **(h)** After recurrent seizure activity nearly half of neurons lose

their inhibitory response to endogenous GABA or switch their inhibitory response from inhibition to excitation.

Table 1

Efficacy of GABAergic anticonvulsants in animal models of neonatal seizures.

#	Preparation/Model	Age (P)	Anticonvulsant (AED)	Concentration	Application	Efficacy	Author(s)
1	<i>In vivo</i> /Flurothyl	9; 15	Phenobarbital	20 mg/kg	Pretreatment (i.p)	High	(Velisek et al., 1995)
2	<i>In vivo</i> /pentylene-tetrazol	7; 12	Clobazam	0.5–7.5 mg/kg	Pretreatment (i.p)	High	(Haugvicova et al., 1999)
3	<i>In vitro</i> /0Mg ²⁺	7–8	Phenobarbital Phenobarbital	30 μM 100 μM	After 3 ILDs	Low High	(Quifichini et al., 2003)
4	<i>In vitro</i> ; <i>in vivo</i> /K ⁺ +gabazine	8–2, 17–21	Diazepam	5μM	Co-injection (before ILD)	High	(Isaev et al., 2007)
5	<i>In vitro</i> /0Mg ²⁺	4–6	Phenobarbital	100 μM	After 7 ILDs	Low	(Dzhala et al., 2008)
6	<i>In vitro</i> /8.5 K ⁺ ; <i>In vivo</i> /Kaimic Acid	5–7; 9–12	Phenobarbital Phenobarbital	100 μM 25 mg/kg	After 7 ILDs Pretreatment (i.p)	Low Modest	(Dzhala et al., 2005)
7	<i>In vivo</i> /Kaimic acid; flurothyl	10 10	Phenobarbital Diazepam	50 mg/kg 4–16 mg/kg	Stage 5 seizures (i.p)	Significant Transient	(Raol et al., 2009)

Table 2

$[Cl^-]_i$ accumulation during low- Mg^{2+} ; induced recurrent seizures.

Seizures	Control			+ Bumetanide				
	$\Delta[Cl^-]_i$ (mM)	n (cells)	IHF	P	$\Delta[Cl^-]_i$ (mM)	n (cells)	IHF	P
1-2	8.1 ± 1.2	187	4	<0.05	6.8 ± 0.8	185	4	<0.05
3-4	11.4 ± 1.2	187	4	<0.05	10.4 ± 1	185	4	<0.05
5-6	17.2 ± 2.7	187	4	<0.05	7.5 ± 0.75	185	4	<0.05
7-8	28 ± 1.8	187	4	<0.05	5.2 ± 0.85	185	4	<0.05

* n represents the number of cells; IHF – number of hippocampi and p values correspond to one-way ANOVA followed by Tukey's means comparison